ERG activity is regulated by endothelial FAK coupling with TRIM25/USP9x in vascular patterning

Gabriela D'Amico[1] #, Isabelle Fernandez[1] † #, Jesús Gómez-Escudero[1] #, Hyojin Kim[2,] §, Eleni Maniati[3,]§, Muhammad Syahmi Azman[4], Faraz K. Mardakheh[4], Bryan Serrels[6], Alan Serrels[7], Maddy Parsons[8], Anthony Squire[9], Graeme M. Birdsey[10], Anna M. Randi[10], Alfonso Bolado-Carrancio[11], Rathi Gangeswaran[5], Louise E. Reynolds[1], Natalia Bodrug[1], Yaohe Wang[5], Jun Wang[4], Pascal Meier[2] and Kairbaan M. Hodivala-Dilke[1,*]

[1] Centre for Tumour Microenvironment Institute of Cancer Research, Chester Beatty Laboratories, Fulham Road, London SW3 6JB, UK
[2]The Breakthrough Toby Robins Breast Cancer Research Centre, Institute of Cancer Research, Chester Beatty Laboratories, Fulham Road, London SW3 6JB, UK
[3]Centre for Cancer Genomics and Computational Biology, Barts Cancer Institute – a CR-UK Centre of Excellence, Queen Mary University of London, John Vane Science Centre, Charterhouse Square, EC1M 6BQ London, UK
[4]Centre for Cancer Cell and Molecular Biology, Barts Cancer Institute – a CR-UK Centre of Excellence, Queen Mary University of London, John Vane Science Centre, Charterhouse Square, EC1M 6BQ London, UK
[5]Centre for Cancer Biomarkers and Biotherapeutics, Barts Cancer Institute – a CR-UK Centre of Excellence, Queen Mary University of London, John Vane Science Centre, Charterhouse Square, EC1M 6BQ London, UK
[6]Institute of Cancer Sciences, University of Glasgow, Garscube Estate, Switchback Road, Bearsden, G61 1QH, UK
[7]Centre for Inflammation Research, Queen's Medical Research Institute, University of Edinburgh, Edinburgh BioQuarter, 47 Little France Crescent, Edinburgh EH16 4TJ, UK
[8]Kings College London, Randall Centre of Cell and Molecular Biophysics, Room 3.22B, New Hunts House, Guys Campus, London, SE1 1UL, UK
[9]IMCES - Imaging Centre Essen, Institute for Experimental Immunology and Imaging, University Clinic Essen Hufelandstrasse 55, 45122 Essen, Germany
[10]National Heart & Lung Institute, Imperial College London, Hammersmith Hospital, Du Cane Road, W12 0NN London, UK
[11]Institute of Genetics and Cancer, University of Edinburgh, UK

[†]Present Address: Institut national du cancer (INCa), Department of Biology, Transfer and Innovation, Research and Innovation Division, 52 avenue André Morizet, 92513 Boulogne-Billancourt Cedex, France
#Equal first-author contribution §Equal second-author contribution
*Corresponding Author: Prof. Kairbaan Hodivala-Dilke (e-mail: k.hodivala-dilke@qmul.ac.uk)

Keywords: **vascular patterning regulation, retinal angiogenesis, endothelial cell signaling**

Abstract

Precise vascular patterning is critical for normal growth and development. The ERG transcription factor drives Delta like ligand 4 (DLL4)/Notch signalling and is thought to act as pivotal regulators of endothelial cell (EC) dynamics and developmental angiogenesis. However, molecular regulation of ERG activity remains obscure. Using a series of EC specific Focal Adhesion Kinase (FAK)-knockout (KO) and point-mutant FAK-knockin mice, we show that loss of ECFAK, its kinase activity or phosphorylation at FAK-Y397, but not

FAK-Y861, reduces ERG and DLL4 expression levels together with concomitant aberrations in vascular patterning. Rapid Immunoprecipitation Mass Spectrometry of Endogenous Proteins identified that endothelial nuclear-FAK interacts with the de-ubiquitinase USP9x and the ubiquitin ligase TRIM25 enzymes. Further *in silico* analysis corroborates that ERG interacts with USP9x and TRIM25. Moreover, ERG levels are reduced in FAKKO ECs via a ubiquitin-mediated post-translational modification programme involving USP9x and TRIM25. Re-expression of ERG *in vivo* and *in vitro* rescues the aberrant vessel sprouting defects observed in the absence of ECFAK. Our findings identify ECFAK as a regulator of retinal vascular patterning by controlling ERG protein degradation via TRIM25/USP9x.

Introduction

The molecular regulation of vascular patterning involves precise control of endothelial cell (EC) proliferation, migration and spatial/temporal organization within growing blood vessels during angiogenic sprouting. Although VEGF-A (vascular endothelial growth factor, VEGF) is a major regulator of vessel patterning, how VEGF signalling intersects with other molecular networks governing these processes *in vivo* is still under investigation(Bautch, 2012). Among the ETS (E-26 transformation-specific) family members, the transcription factor ERG (ETS-related gene) is a central regulator of EC specification and homeostasis in angiogenesis(Shah et al., 2016). Whilst downstream of VEGF signalling by the Delta-like 4 (DLL4) Notch ligand coordinates the dynamic spatial competition between ECs for a leading position at the tip of vessel sprout, a process that is thought to be essential in promoting correct patterning(Blanco and Gerhardt, 2013, Jakobsson et al., 2010), the transcriptional regulation of DLL4 expression has been reported to be associated with ERG levels and activity(Wythe et al., 2013, Fish et al., 2017, Shah et al.,

2017). However, identification of upstream molecular regulators of ERG expression and function in EC migration and angiogenesis is under-explored.

Focal adhesion kinase (FAK), also known as protein tyrosine kinase 2 (PTK2), is a non-receptor protein tyrosine kinase which acts on downstream cell surface receptors, including VEGF receptors, to transduce their signals and has been implicated as essential in EC migration, proliferation, survival and developmental angiogenesis(Mitra et al., 2005, Schaller, 2010, Braren et al., 2006, Shen et al., 2005). ATP binding to the FAK-kinase domain induces phosphorylation at tyrosine (Y) 397 and subsequent phosphorylation at Y861. ECFAK-kinase dead embryos and global loss of FAK exon 15, that encodes the Y397 region of FAK, display severe vascular defects(Corsi et al., 2009, Zhao et al., 2010, Lim et al., 2010) whilst phosphorylation of Y861 is proposed to be required for *in vitro* VEGF-induced angiogenesis(Abu-Ghazaleh et al., 2001). Despite these results the specific roles of ECFAK kinase activity and phosphorylation at FAK-Y397 and FAK-Y861 in vascular patterning *in vivo* are not clear. To date much of ECFAK research has focused on its role at focal adhesions and its cytoplasmic signaling functions. More recently FAK was described to translocate from the cytoplasmic compartment to the nucleus(Lim, 2013; Sun et al. 2018). Even though FAK seems to be able to regulate expression of target genes by binding to transcription factors in several cell types, this has not been extensively studied in ECs and its mechanisms are not well understood. Thus, understanding how FAK expression and activity might regulate ERG could reveal the molecular orchestration of vascular patterning.

In this study, we describe that nuclear ECFAK acts as an upstream regulator of ERG. ERG expression, via ubiquitin-regulated post-translational modifications, is controlled by nuclear ECFAK association with the de-ubiquitinase USP9x and the ubiquitin ligase TRIM25 enzymes. The loss of ECFAK expression, and loss of its kinase activity, or ECFAK-phosphorylation at tyrosine 397, but not at tyrosine 861, all disrupt vessel patterning *in vivo*

with a concomitant reduction in ERG and DLL4 expression. EC-tip cell positioning and migration is also abrogated by loss of ECFAK expression, kinase activity or phosphorylation of FAK at tyrosine 397, whereas the overexpression of ERG *in vivo* and *in vitro* rescues the loss of FAK-knockout phenotypes. Overall, our findings identify that nuclear ECFAK regulates TRIM25 and USP9x in the control of ERG expression providing a FAK-meditated mechanism for vascular patterning control.

Results

ERG expression and vascular patterning are controlled by endothelial cell FAK

FAK flox/flox mice were crossed with mice expressing a tamoxifen-inducible Cre deleter (iCreERT2) that is driven by endothelial cell (EC)-selective platelet-derived growth factor subunit B (*Pdgfb*) promoter (*Pdgfb-iCreERT2*) (Tavora et al., 2010). Mice without Cre were used as control (*Pdfgb-iCre*^{ERT}-;FAK fl/fl). To induce EC restricted FAK deletion, we injected 4-hydroxytamoxifen (4-OHT) from postnatal day 1 (P1) to P2 and isolated primary ECs from lungs at P10-P14. Molecular signalling events modulated by ECFAK loss, in the context of VEGF stimulation, were examined to identify putative regulators of vascular patterning. Using isobaric tandem mass tagging (TMT) based quantitative proteomic and phospho-proteomics (**Fig. S1, A and B**), 86 proteins were commonly differentially expressed (DE) between wild-type (FAK^{WT}) and FAK-knockout (FAK^{KO}) ECs in control (PBS) and VEGF-stimulated conditions (**Fig. 1, A)**. Loss of ECFAK (PTK2) was confirmed and pointed towards putative VEGF-stimulated pathways regulated by ECFAK (**Fig. 1, B**). Specifically, protein category enrichment analysis revealed that FAK-deficiency caused an increase in protein categories which reflect cytoplasmic canonical FAK functions, but a decrease in protein categories that reflect nuclear non-canonical FAK functions (**Fig. 1, C and Fig. S1, C and D**). Furthermore, hierarchical clustering of the common significantly DE proteins

verified the loss of FAK (also known as PTK2) in FAK^{KO} ECs and identified a significant downregulation of ERG in FAK^{KO} ECs after VEGF-stimulation (**Fig. 1, D**). Protein category enrichment analysis of the phospho-proteome revealed a similar decrease of nuclear non-canonical FAK functions (**Fig. S1, E to G**). ERG expression levels were reduced in primary FAK^{KO} lung ECs (**Fig. S2, A to D**). Together, these findings established that loss of EC FAK modulates ERG protein expression.

Previous research has shown ERG to play a role in retinal angiogenesis (Birdsey et al., 2015, Shah et al., 2017, Fish et al., 2017), a well-established model to study sprouting and vascular patterning *in vivo* (Blanco and Gerhardt, 2013). Corroborating our previous results, a significant reduction of *in vivo* ERG expression was observed in $ECFAK^{KO}$ retinal vasculature tip cells, stalk cells and total vascular front compared with $ECFAK^{WT}$ controls (**Fig. 1, E and Fig. S2, E**). Furthermore, the morphology of retinal vessels in $ECFAK^{KO}$ mice was significantly compromised showing reduced vascular outgrowth, reduced number of sprouts and sprout length, together with increased number of filopodial extensions and reduced EC proliferation (**Fig. 1, F and Fig. S2F**). Overall, the loss of ECFAK expression resulted in reduced ERG expression *in vivo* and *in vitro* and this correlated with aberrant retinal vascular patterning.

To determine whether FAK-kinase activity and/or phosphorylation of FAK at tyrosine (Y) 397 and/or 861 regulates ERG expression and retinal angiogenesis we next examined the effect of inducible EC-specific point-mutations in: (1) FAK-kinase dead mutant ($ECFAK^{KD}$) mice, in which FAK catalytic activity is abolished by a K454R mutation; (2) non-phosphorylatable Y397 ($ECFAK^{Y397F}$) mice and (3) non-phosphorylatable Y861 ($ECFAK^{Y861F}$) mice(Alexopoulou et al., 2017, Pedrosa et al., 2019, Newport et al.,2021). Wild-type FAK knockin mice ($ECFAK^{KIWT}$) were used as controls. The Cre-inducible system for mutant FAK expression was generated by designing mutant chicken-FAK constructs

(preceded by a STOP sequence flanked by loxP sites) that were targeted to the ubiquitous Rosa26 locus (R26FAKKI/KI) (Tavora et al., 2014). R26FAKKI/KI mice were bred with the inducible endothelial-specific FAK knockout mice we previously used. Administration of 4-OHT lead to simultaneous deletion of the endogenous mouse-FAK gene and the neoSTOP cassette thus allowing the homozygous expression of the mutated chicken-FAK transgene: wild-type (KI WT), kinase dead (KD), non-phosphorylatable Y397 (Y397F) or non-phosphorylatable Y861 (Y861F) knockin-chicken-FAK expression specifically in endothelial cells to generate: ECFAK$^{KI\ WT}$, ECFAK^{KD,} ECFAK^{Y397F} and ECFAK^{Y861F} mice, respectively. Analysis of the retinal vasculature at P6 revealed that vascular outgrowth, numbers and length of sprouts were all reduced in ECFAK^{KD} and ECFAK^{Y397F} but not in ECFAK^{Y861F} mutants (**Fig. 2, A and B**). Additionally, the number of filopodia at the vascular front was increased significantly in both ECFAK^{KD} and ECFAK^{Y397F}, but not in ECFAK^{Y861F} mice, when compared with ECFAK^{KIWT} controls (**Fig. 2, C**). Concomitantly, ERG expression was reduced in ECFAK^{KD}, ECFAK^{Y397F}, but not ECFAK^{Y861F} retinal vasculature (**Fig. 2, D**). These *in vivo* data were also supported by reduced Erg mRNA levels in FAK^{KD} and FAK^{Y397F}, but not FAK^{Y861F}, primary ECs from P6 pups (**Fig. S2, G**). EC-specific mutant FAK-knockin system validation was performed **(Fig. S3)**. Together, these data suggest that physiological FAK expression and, in particular, FAK kinase-activity and phosphorylation at Y397 are required for ERG regulation in the control of retinal vascular patterning.

DLL4/Notch signalling and sprouting depends on endothelial-cell FAK

Since transcriptional regulation of DLL4 has been associated with ERG activity(Wythe et al., 2013, Fish et al., 2017, Shah et al., 2017), we next sought to investigate the expression of DLL4 in the ECFAK-mutant mice. Whilst DLL4 decorated the ECs at the vascular front in ECFAK^{WT} retinas, a significant reduction in DLL4 protein expression levels was observed in

ECFAK^{KO}, ECFAK^{KD} and ECFAK^{Y397F}, but not ECFAK^{Y861F} retinas (**Fig. 3, A and B; Fig. S4, A to F**). In line with this, transcripts for *Fak* and several Notch signalling effectors, including *Dll4*, *Hey1*, *Hey2*, and *Nrarp* were reduced in FAK^{KO} ECs (**Fig. S4, G)**. Furthermore, Notch receptor intracellular domain (NICD) expression levels, which reflects ligand-dependent activation of Notch signalling(Blanco and Gerhardt, 2013), were also reduced in FAK^{KO} ECs (**Fig. S4, G to I**). Together these data indicate that the loss of ECFAK expression, ECFAK-kinase activity and phosphorylation at FAK-Y397 reduce DLL4 expression similarly to the reduction in ERG expression.

To investigate whether the ECFAK-mediated control of ERG and DLL4 expression was associated with functional changes in EC spatial organization within vascular sprouts, fluorescent colour-dye prelabelled control primary ECs in green (FAK^{WT} or FAK^{KIWT}) and prelabelled primary FAK-mutant ECs in red (FAK^{WT}, FAK^{KIWT}, FAK^{KO}, FAK^{KD}, FAK^{Y397F} or FAK^{Y861F}) were used in 2D and 3D competition assays. Results indicated that FAK^{KO}, FAK^{KD} and FAK^{Y397F} ECs but not FAK^{Y861F} ECs have a significant disadvantage to locate at the tip cell position in the 3D sprouting competition assays (**Fig. 3, C and D**). Additionally, both FAK^{KD} and FAK^{Y397F} ECs, but not FAK^{Y861F}, ECs showed a significant decrease in 2D directed chemotaxis behaviour when in presence of FAK^{KIWT} cells **(Fig. 3, E**). Overall, our data suggest that the reduction in ERG and DLL4, together with the reduction in FAK levels and, importantly, FAK-kinase activity as well as phosphorylation at Y397, but not at Y861, are involved in establishing endothelial tip-stalk cell fate and/or its precise spatial organization of EC within vessel sprouts.

Nuclear endothelial-cell FAK interactome with ERG-associated USP9x and TRIM25

We next sought to identify the molecular mechanism of ERG regulation by FAK in ECs. FAK has been reported to function both in the cytoplasm and also in the nucleus, where it has

DNA-binding roles(Lim, 2013). Relevant to our study, published work demonstrates that ERG-dependent dynamic induction of DLL4 transcription in human umbilical vein EC *in vitro* peaks at 30 min of VEGF stimulation(Fish et al., 2017). Therefore, we analysed nuclear and cytoplasmic primary mouse EC fractions after VEGF stimulation for 30 min and found that full-length wild-type FAK translocates to the nucleus and that phosphorylated FAK can also translocate to the nucleus in FAK^{KIWT}, FAK^{Y861} FAK^{KD} and FAK^{Y397F} ECs (**Fig S5, A to C**) confirming previous reports of the nuclear translocation of FAK despite the lack of its kinase function (Lim, 2013).

Rapid Immunoprecipitation Mass spectrometry of Endogenous proteins (RIME)(Mohammed et al., 2016), was applied to human ECs (HUVEC) treated with either PBS or VEGF to analyse FAK interactors **(Fig. S6, A**). From the approximately 500 nuclear FAK-specific interactors were identified Using TRRUSTv2 and Qiagen database interrogation, 24 of the nuclear FAK-specific interactors identified by RIME analysis were experimentally predicted to interact with ERG (**Fig 4, A and B**). These included two protein-protein interactions with: (1) the de-ubiquitinase USP9x, and (2) the ubiquitin ligase TRIM25, which have both been reported promote ERG stabilization and ERG degradation, respectively, in cancer cells (Wang et al., 2014, Wang et al., 2016).

Endothelial cell FAK regulates ERG expression via ubiquitinylation

To test the functional requirement of USP9x and TRIM25 in ERG expression in FAK^{WT} and FAK^{KO} USP9x and TRIM25 were depleted in FAK^{WT} and FAK^{KO} ECs using CRISPR/Cas9-gene editing approach. USP9x depletion (gUSP9x) reduced total ERG expression levels, compared with genotype-matched gControl, in both FAK^{WT} and FAK^{KO} ECs (**Fig. 4, C**). In contrast, TRIM25 depletion (gTRIM25) caused an upregulation of total ERG expression levels compared with gControl in FAK^{WT} cells, but a downregulation of ERG expression

levels compared with ERG expression levels in gControl FAK^{KO} ECs. Since USP9x is a de-ubiquitinase enzyme and TRIM25 a ubiquitin ligase enzyme, the overall ubiquitination status of ERG was next assessed to test the possible link with ERG expression regulation by proteosomal degradation. Immunoprecipitation of ubiquitinylated proteins (UBI) in the presence of proteasome inhibitor MG132, that is known to repress protein degradation allowing accumulation of ubiquitinylated proteins, followed by western blotting for ERG showed that ubiquitinylation of ERG is enhanced significantly in FAK^{KO} compared with FAK ^{WT} ECs and suggests that FAK modulates ERG protein degradation (**Fig. 4, D**). Additionally, treatment with the MG132 for 4 hours also rescued the levels of ERG in FAK^{KO} ECs to similar levels as in FAK^{WT} ECs (**Fig 4, E**). Thus, FAK contributes to regulating protein expression levels of ERG through modulation of ubiquitylation and de-ubiquitylation by USP9X and TRIM25.

ERG re-expression restores DLL4 levels and FAK-dependent vessel patterning phenotypes

The functional requirement of ERG in FAK-regulated vascular patterning was next assessed. ECFAK^{WT} and ECFAK^{KO} newborn pups were injected at P1(Klose et al., 2015)with an ERG adenovirus, either Ad-ERG-V5(Sperone et al., 2011) or Ad-LacZ-V5 as control. Although Ad-LacZ-V5 infection had no overt effects, restoration of ERG expression by Ad-ERG-V5 infection resulted in a significant rescue of both DLL4 expression and vessel outgrowth in ECFAK^{KO} mice. Likewise, Ad-ERG-V5 infection of ECFAK^{KD} and ECFAK^{Y397F} mutants restored both ERG and DLL4 levels back to that found in control pups and restored the vascular outgrowth phenotypes in these mice (**Fig. S7, A to D**). Conversely, depleting ERG expression, using ERG-targeted siRNA *in vitro,* in primary ECs from ECFAK^{Y861F} newborns, showed a reduction in *Dll4* expression but not *Pecam1* confirming a regulation of DLL4 by ERG in FAK^{Y861F} mutant ECs (**Fig. S7, E**). Validation of the experimental system was

confirmed using Ad-Cre viruses in $FAK^{flox/flox}$ pups (**Fig. S8**). Lastly, ERG over-expression (pERG)(Sperone et al., 2011) in FAK^{KO} ECs (pERG-FAK^{KO}) rescued the compromised tip cell position phenotype caused upon FAK deletion (pControl-FAK^{KO}) (**Fig. 5, E and F**) and the reduced VEGF-mediated migratory responses phenotype in these cells (**Fig. 5, G to I**). Altogether, ERG re-expression restores DLL4 levels, migration, tip cell positioning and FAK-mediated vessel patterning phenotypes *in vivo* and *in vitro.*

Discussion

In short, we identified a fundamental mechanism in the control of vascular patterning via endothelial-cell nuclear FAK-USP9x and -TRIM25 interactions in the regulation of ERG expression by ubiquitinylation. ERG expression is controlled by ECFAK and its kinase activity. Our data indicate that nuclear ECFAK-USP9x/TRIM25-ERG-DLL4 regulates the control of Notch activity thus governing endothelial tip and stalk cell positioning and vascular patterning (Blanco and Gerhardt, 2013, Jakobsson et al., 2010, Ubezio et al., 2016, Shah et al, 2017) (**Fig 5, J**).

The current understanding of the regulation of ERG expression is still in its infancy. The ERG gene is also known to be fused to TMPRSS2 (Transmembrane Protease Serine 2) in prostate cancer cells resulting in ERG overexpression. Although recent studies revealed that E3 ubiquitin ligases, such as SPOP and TRIM25, interact specifically with and promote ubiquitination and degradation of oncogenic ERG protein (Wang et al., 2016, Gan et al., 2015); whether either SPOP or TRIM25 regulates physiological ERG levels in endothelial cells was unclear. A recent study has shown that Casein kinase I phosphorylates ERG to promote SPOP/ERG interaction and thus degradation of oncogenic ERG(Gan et al., 2015). Interestingly, it has been described in prostate cancer cells the de-ubiquitanase enzyme USP9X, interacts with ERG and promotes its stabilization to decrease prostate cancer cell

proliferation (Wang et al, 2014). Our data identify that nuclear ECFAK interacts with TRIM25 and USP9X, which is relevant in the regulation of ERG proteasomal ubiquitinylation and the control of ERG protein levels in endothelial cells and vessel patterning.

Our study suggests that loss of ECFAK, its kinase activity, or phosphorylation at FAK-Y397 are all sufficient to reduce sprouting angiogenesis in the mouse retina whilst increasing filopodial extensions. The basis of these vascular patterning defects associated not only with reduced ERG expression but also with reduced DLL4 expression, reduced EC migration and competition for the tip cell position at the distal end of vessel sprouts. Thus, the ECFAK phenotype seems to recapitulate some, but not all, of the phenotypes in DLL4 haploinsufficient mice or those treated with pharmacological inhibitors of DLL4/Notch pathway. For example, the increase in filopodia observed in our mutant mice was also observed in DLL4 haploinsufficient mice(Blanco and Gerhardt, 2013, Jakobsson et al., 2010). However, the blunted vascular front with associated reduction in vessel sprouts was not expected. These apparent differences might be explained by a recent report showing that DLL4 expression is actually dynamic within ECs of the vascular sprout, and that synchronization of DLL4 oscillations switches from a sprouting to a non-sprouting, expanding phenotype(Ubezio et al., 2016). Most interestingly, the activity of transcription factors can be influenced by their own turnover as shown for estrogen receptor-alpha or c-MYC(Gierisch et al., 2016). Given that ECFAK affects ERG expression and regulation of DLL4 (Wythe et al., 2013, Fish et al., 2017, Shah et al., 2017), this likely represents a mechanism for the regulation of vascular patterning in the absence of ECFAK or its kinase functions.

Our study advances our understanding of the basic mechanisms and concepts of vascular biology but may also have clinical relevance to FAK expression in some human eye disorders. Pathological angiogenesis is the underlying basis of many ocular diseases such as retinopathy of prematurity, proliferative diabetic retinopathy and wet age-related macular degeneration. Published work has shown that FAK gene expression levels change during aging of human neural retina(Cai et al., 2012) and FAK protein and phosphorylation levels are overexpressed in human uveal melanomas(Faingold et al., 2014). However, the specific role of endothelial FAK and/or phosphorylation level are currently unknown. Norrie disease and familial exudative vitreoretinopathy (FEVR) are both hereditary eye disorders characterized by aberrant and incomplete retinal vascular development, and are associated with mutations in Fzd4(Junge et al., 2009) which has been linked to ERG expression in other angiogenesis-associated disease(Gupta et al., 2010). Moreover, ERG expression is lost in other pathological diseases as atherosclerosis (Sperone et al. 2011), chronic liver disease (Dufton, Nat Comms 2017) and pulmonary arterial hypertension (PAH) (Looney et al. 2017). Whether endothelial FAK role in ERG expression regulation is implicated in those contexts remains to be established.

Materials and Methods

Study and Experimental Design

This is a controlled laboratory study using mice. The mouse-based study involved in vivo and in vitro techniques. Mice were administered 4-hydroxy-tamoxifen (4-OHT) to induce chicken FAK (wild type and mutant) expression in endothelial cells. Whole mouse litters from each strain/colony were treated and processed. Mice with specific genotypes were enrolled into the experimental study. The treatment of pups with 4-OHT or Adenoviruses - to induce deletion/mutation or expressing target proteins respectively, as well as the weighing, dissection of tissues were all blinded procedures. Imaging and analyses were all performed in a blinded fashion manner. Samples sizes were based on previous experience and published

work. Samples from pups and/or cells where transgenic inductions (deletions/knockin) failed (e.g., endogenous FAK deletion/mutated FAK ratio was not satisfactory by mRNA and protein analysis) were not included for analysis in this study. N-number for experiments, sample size and experimental replicates are stated in Figure Legends and Material and Methods.

Mice Breeding and Procedures

FAK conditional-knockout and -knockin mouse models were generated as previously described(Newport et al., 2021; Alexopoulou et al., 2017, Pedrosa et al., 2019, Tavora et al., 2014, Tavora et al., 2010) FAKfl/fl mice were crossed with inducible endothelial-specific Cre transgenic deleter line: *PdgfbiCre*ERT(Claxton et al., 2008) to generate *PdgfbiCre*ERT;FAKfl/fl and additionally crossed with R26FAK$^{KI/KI}$: R26FAK$^{KIWT/KIWT}$, R26FAK$^{KD/KD}$, R26FAK$^{Y397F/Y397F}$ and R26FAK$^{Y861F/Y861F}$ to generate *PdgfbiCre*ERT;FAKfl/fl; R26FAK$^{KI/KI}$ mice (see Table 1 for mice nomenclature). All mice used were maintained on a mixed C57BL6/129 genetic background. The endothelial FAK-deletion and FAK-KI mutations were induced by treatment with 4-OH-tamoxifen (4-OHT, #H7904, Sigma; in a mixed solution of ethanol/sunflower oil of 1:10). Unless otherwise stated, 20 μl/g of a solution at 3.3 mg/mL was injected intragastrically in newborn mice at postanatal P1 and P2. Mice were humanely sacrificed and examined at P6 and P10-14. All experiments were conducted using littermate controls. Husbandry and experiments were performed in accordance with the UK Animals (Scientific Procedures) Act 1986 regulations, under Home Office Project License No. PF220CE02.

Genotyping PCR

Genotyping of *PdgfbiCre*ERT;FAKfl/fl and *PdgfbiCre*ERT;FAKfl/fl; R26FAK$^{KI/KI}$ mice was performed using DNA isolated from ear or tail snips with primers and protocols previously published(Tavora et al., 2014).

Adenovirus and Rescue Experiments *in vivo*

ERG expression was carried out using a V5-tagged ERG-3 adenovirus (AdERG), described previously(Sperone et al., 2011). A β-galactosidase adenovirus (AdLacZ) was used as control. Large-scale production of high-capacity adenoviruses were performed as previously published(Wang et al., 2003). Newborn mice from *PdgfbiCre*ERT;FAKfl/fl; *Pdgfb-iCre*ERT;FAKfl/fl; R26FAK$^{KD/KD}$ and *PdgfbiCre*ERT;FAKfl/fl; R26FAK$^{Y397F/Y397F}$ were intraperitoneally injected with 1×10^8 PFU at P1. Subsequently, the pups were intragastrically injected with 4-OHT (solution/volumes as described above) at P2 and P3, to induce the endogenous FAK deletion and, for the knockin strains, the simultaneous chicken FAK mutated expression. At P6 pups were sacrificed by cervical disslocation and tissues including whole eyes, lungs and livers were collected for analysis. Two litters for each adeno-treated group per mice strain were utilized to obtain no less than four mice per condition.

Whole-mount immunofluorescence analysis of mouse retinas

Whole eyes were collected from ECFAK^{KO} and ECFAK^{KI} mice at P6. Retinas were dissected and processed for whole-mount immunofluorescence staining as described previously(Pitulescu et al., 2010). Briefly, whole eyes were fixed with freshly prepared 4% paraformaldehyde (PFA) in PBS for up to 6 h at 4^{o}C on a rocking platform. Retinas were dissected and blocked/permeabilized in Claudio Blocking Buffer (CBB) (Franco et al., 2015)

for 2 h at room temperature, then incubated overnight on a rocking platform at 4°C in 1:1 CBB plus rabbit-anti-ERG (1:200, #ab9251, Abcam) and goat anti-DLL4 antibodies (1:100, #AF1389, R&D). After washing several times in PBS at room temperature, retinas were incubated overnight at 4°C in 1:1 CBB plus donkey anti-rabbit AlexaFluor 647 and donkey-anti-goat AlexaFluor 555 antibodies (1:300, #A-31573 and #A-21432, ThermoFisher Scientific). After washing several times in PBS at room temperature, retinas were post-fixed in 1% PFA for 2 min, rinsed in PBS, washed twice in PBLEC buffer (1% Triton X-100, 0.1 mM $MgCl_2$, 0.1 mM $CaCl_2$, 0.1 mM $MnCl_2$ in PBS pH 6.8), re-blocked in 1% BSA and 0.5% Triton X-100 in PBS for 1 h and incubated overnight in PBLEC plus biotinylated *Griffonia Simplicifolia* Lectin I Isolectin B4 (IB4, 1:25, #B-1205, Vector Laboratories). After further washes in in PBS, retinas were incubated overnight on a rocking platform in 0.5% BSA and 0.3% Triton X-100 in PBS plus streptavidin AlexaFluor 488 (1:100, #S11223, ThermoFisher Scientific). Retinas were washed several times in PBS, further stained with Hoechst 33342 in PBS (1:5000, #H3570, ThermoFisher Scientific) for 30 min at room temperature, rinsed in PBS twice, post-fixed in 1% PFA for 2 min, further washed in PBS and flat-mounted on glass microscope slides using ProLong Gold anti-fade mounting medium (ThermoFisher Scientific). Confocal microscopy imaging was carried out using Carl Zeiss LSM710 and LSM 880 AiryScan microscopes.

EdU labelling of proliferating endothelial cells

For detection of proliferating endothelial cells *in vivo* in $ECFAK^{KO}$ mice, a stock of 1 mg of 5-ethynyl-2'-deoxyuridine (EdU) (#A10044, ThermoFisher Scientific) was dissolved in a 10% DMSO/PBS solution; 10 µl of this stock solution/gram of body weight was injected intraperitoneally 4 h before the mice were sacrificed. Whole eyes were collected and processed as described above. Retinas were dissected and permeabilized for 2 h at room

temperature with 0.5% Triton X-100 in PBS. EdU-positive cells were detected with the Click-iT EdU AlexaFluor 647 Imaging Kit (#C10340, ThermoFisher Scientific). Endothelial cells were detected by ERG and IB4 immunofluorescence staining as described above but using donkey anti-rabbit AlexaFluor 594 as secondary antibody for ERG detection instead (#R37121, ThermoFisher Scientific). Confocal microscopy imaging was carried out using Carl Zeiss LSM710.

Anti-Adenovirus Hexon protein immunohistochemistry

Paraformaldehyde paraffin embedded liver histological sections from P6 ECFAK^{WT} and ECFAK^{KO} mice that were transduced with Adeno-ERG or Adeno-LacZ were used. Tissue sections were de-waxed, rehydrated through graded alcohols and pre-treated with trypsin enzymatic antigen retrieval solution before immunohistochemistry. Tissue sections were stained using adenovirus Hexon protein antibody (#ab8249, Abcam) and appropriate secondary HRP-conjugated antibody VECTASTAIN Elite ABC reagent (Vector Laboratories) with liquid DAB+ substrate. Imaging was performed using Axiophoto microscope equipped with Zeiss AxioCam HRC and associated AxioVision Rel 4.8 software, using 20x/0,50 Ph2 objectives.

Endothelial cell preparations

Primary mouse lung endothelial cell (MLEC) isolation from ECFAK^{WT}, ECFAK^{KO}, ECFAK^{KIWT}, ECFAK^{KD}, ECFAK^{Y397F} and ECFAK^{Y861F} pups at P6 was performed as previously described(Reynolds and Hodivala-Dilke, 2006) with some modifications. Briefly, lungs from pups that were tamoxifen induced at P1 and P2 to achieve FAK-deletion and FAK point-mutation expression were excised at P6. Lungs from pups with the same genotype were pooled (2-4 lungs/genotype), minced and digested for 1 h at 37°C with Collagenase

type-1 (#17100017, ThermoFisher Scientific), passed through a 70 μm pore size cell strainer (BD Falcon) into MLEC growth media and plated onto tissue culture plates coated with 0.1% gelatin, 10 μg/ml human plasma fibronectin (FC010, Millipore) and 30 μg/ml collagen (C3867, Sigma) and incubated for overnight at 37°C and 5% CO_2. A single positive-sort for EC enrichment was performed using rat anti-mouse monoclonal CD102/ICAM2 (3C4 mlC2/4, #555326, BD Pharmingen) and CD31/PECAM1 (MEC13.3, #550274, BD Pharmingen) antibodies together and sheep anti-rat Dynabeads (#11035, ThermoFisher Scientific). Unless otherwise stated, MLEC were used freshly isolated without further culture for experiments. MLEC growth media is composed of one part Dulbecco's Modified Eagle's Medium low glucose (D-MEM, #21885-025, Gibco), one part Ham's F12 medium (#N6658, Sigma), supplemented with 0.1 mg/ml heparin (#H3149, Sigma), 100 μg/ml penicillin/streptomycin (#P4333, Gibco), 6 mM L-glutamine (#25030-081, Gibco), 20% Fetal Bovine Serum (heat inactivated) (#AXB 32773, HyClone) and 50 μg/ml endothelial mitogen (#J645516, Alfa Aesar). Immortalized MLEC from ECFAK^{WT}, ECFAK^{KO}, ECFAK^{KIWT}, ECFAK^{KD}, ECFAK^{Y397F} and ECFAK^{Y861F} mice were described previously(Alexopoulou et al., 2017, Pedrosa et al., 2019, Tavora et al., 2010).

Immunofluorescence in primary endothelial cells

Freshly isolated primary MLEC from ECFAK^{WT} and ECFAK^{KO} were seeded in MLEC growth media at 20,000 cells/10 mm^2 density onto glass coverslips coated as described above. Cells were left to attach for 4h-overnight at 37°C and 5% CO_2, fixed in 4% PFA for 7 min at room temperature and washed 3 times in PBS; permeabilized with 0.1% Triton-X100 in PBS for 10 min; cells were washed 3 times in PBS and blocked with 1% BSA in PBS for 30 min at room temperature. Primary antibodies were diluted in PBS and incubated for 1h at room temperature: mouse-anti FAK (Clone 77, 1:100, #610287, BD Pharmingen), rat anti-

CD144/VE-cadherin/CDH5 (Clone 11D4.1, 1:100, #555289, BD Pharmingen), goat-anti-DLL4 antibodies (1:100, #AF1389, R&D), rabbit-anti-ERG (1:100, #ab9251, Abcam). Cells were washed 3 times in PBS and incubated with the corresponding secondary antibodies: donkey anti-mouse AlexaFluor 647, donkey anti-rat AlexaFluor 488, donkey-anti-goat AlexaFluor 555 antibodies and donkey anti-rabbit AlexaFluor 647 (1:250, #A-31571, #A-31573, #A-21208 and #A-21432, all from ThermoFisher Scientific) for 30 min at room temperature. After 3 washes in PBS the coverslips were mounted onto microscope glass-slides using ProLong Gold Antifade reagent with DAPI (#P36931, Molecular Probes). Confocal microscopy imaging was carried out using Carl Zeiss LSM710.

Microscopy and retinal vasculature quantification analysis

Fluorescently labelled samples (flat whole-mount retinas and MLEC) were analyzed using confocal microscopes (Zeiss LSM LSM710 or Zeiss LSM LSM880 Airyscan) objectives ×10 with NA 0.45, oil objectives ×40 with NA 1.3 and ×63 with NA 1.4. Images were acquired using the multi-channel fluorescent in frame mode, multi-tile and/or z-stack modules. Composites from up to four fluorescent channels, maximum intensity projections and tile stitching of images were created and analysed employing the readily available 3D visualization and analysis software package Imaris (Bitplane AG), together with the open source image processing and visualization software packages, ImageJ (Fiji distribution, National Institutes of Health, Bethesda, MD, U.S.A.) and CellProfiler (Broad Institute of MIT and Harvard U.S.A.) as indicated below. All quantitations were done across littermates.

The quantitation of various vascular morphometric parameters such as plexus outgrowth, sprout number and length and filopodial number was performed manually as previously described(Lobov et al., 2007, Franco et al., 2015, Pitulescu et al., 2010). For filopodia the

number were normalized to the length of the vascular front. The vascular surface area in retinas was quantified as the IB4-positive area from confocal micrographs acquired from all intact quarters of the processed retinas and at a similar distance from the optic stalk, using the Fiji software.

Endothelial DLL4 expression was quantified by thresholding the area of the DLL4 signals that were IB4 positive from × 40 confocal micrographs acquired from the angiogenic fronts of the retinas. These were expressed relative to the total vascular surface area quantified as described above by IB4. Similarly, DLL4 staining was quantified using Imaris software (Area Volume).

ERG expression in the tip and stalk/capillary cells was quantified using a combination of an in-house written script and pipeline for Fiji and Cellprofiler respectively. The mean ERG expression intensity in each nucleus was calculated by dividing its 3D integrated intensity (after background subtraction) by its equivalent ellipsoid volume. For this an intensity integration along the axial (Z) direction was first obtained using Fiji, by performing a sum projection of the ERG image stacks. The resulting 2D SUM images were then processed using a CellProfiler pipeline to automatically and individually segment and quantify each ERG positive nucleus, both in terms of intensity and shape. Thus providing a subsequent lateral intensity integration (XY) for each nucleus, as well as providing the long and short axis length of a fitted ellipse, equivalent in area to the segmented nuclei. The estimated nuclei volumes for each ERG positive nucleus were then obtained from the volumes of their matching ellipsoids using the standard volume formula $4/3.\pi.a.b^2$, where a and b are the long and short axis lengths respectively. For automated differential analysis, the Cellprofiler

pipeline also enabled the manual selection of ERG positive nuclei residing in the tip of IB4 positive vasculature, relative to ERG nuclei residing in the vascular stems.

Retinal endothelial cell proliferation was examined by quantifying the number of double EdU- and ERG-positive cells - well known proliferative and endothelial cell nuclear markers, respectively - relative to the total ERG-positive endothelial cell nuclei present in the angiogenic vascular front from retina identified by IB4-positivity.

Quantitative real-time PCR analysis

Freshly isolated primary MLEC and tissues including retinas, lungs and livers from ECFAK^{WT}, ECFAK^{KO}, ECFAK^{KIWT}, ECFAK^{KD}, ECFAK^{Y397F} and ECFAK^{Y861F} pups at P6 were lysed in RLT buffer (Qiagen). Total mRNA was isolated using the RNAEasy Mini kit (Qiagen). Quality control and concentration of samples was carried out using a Nanodrop ND-10000 spectrophotometer. RNA was reverse transcribed using High Capacity cDNA Reverse Transcription kit (Applied Biosystems) according to the manufacturer instructions. Real-time PCR was performed in a StepOne Plus thermocycler (Applied Biosystems) using TaqMan Master mix and primers custom-made that were specific to mouse *Fak* or chicken *Fak*(Tavora et al., 2014), *Dll4* (Mm00444619_m1), *Nrarp* (Mm00482529_s1), *Hey1* (Mm00468865_m1), *Hey2* (Mm00469280_m1), *Erg* (Mm01214244_m1), *Pecam1/CD31* (Mm01246167_m1) and *Gapdh* (4352339E) all from Applied Biosystems). The data were normalized to *Gapdh* endogenous control to compensate for experimental variations, and for retina tissue also to *Pecam1*, to compensate for alterations in endothelial cell numbers. Fold changes were calculated using the comparative CT (cycle threshold) method. For validation of adenoviral transduction in livers, qRT-PCR analysis was performed using PerfeCTa SYBR Green Fastmix (Quanta Biosciences) reagents and Erg–V5 F and Erg–V5 R primers that span

the region across the Erg-V5 fusion and gene expression values were normalized to mouse *Hprt* endogenous control (primer sequences were published previously(Sperone et al., 2011).

Immunoblotting analysis

Unless otherwise indicated, protein from freshly isolated primary MLEC from ECFAK^{KO} pups was extracted in RIPA lysis buffer (#20-188, Millipore) supplemented with protease inhibitor cocktail set I (#539131, Calbiochem). Proteins from PMT from ECFAK^{KO} and ECFAK^{KI} mice were extracted in lysis buffer (3% SDS, 60 mM Sucrose, 65 mM Tris-HCl, pH 6.8). Samples were sonicated and protein concentration was determined with DC Protein Assay (Bio-Rad). Lysates were heated in NuPAGE LDS sample buffer (ThermoFisher Scientific) at 70°C for 10 min before loading onto 10% acrylamide gels. 15-30 µg of protein was analyzed by SDS-PAGE. After migration, proteins were transferred to a nitrocellulose membrane (Protran BA85, 0.45 µm; GE Healthcare Life Sciences) that was blocked with 5% non-fat milk in Tris-buffered saline with 0.1% Tween-20 (TBS-T) for 1 h at room temperature and incubated overnight at 4^{o}C with primary antibodies diluted in 4% BSA in TBS-T: FAK (Clone 77, 1:1000, #610287, BD Pharmingen), DLL4 (1:1000, #AF1389 R&D), Myc-tag clone 9E10 (1:1000, #ab206486, Abcam), pY397-FAK (1:1000, #3283, CST), pY861-FAK (1:1000, #PS1008, Invitrogen) and HSC70 (1: 5000, #sc-7298, Santa Cruz). For ERG (1:500, #ab9251, Abcam) and GAPDH (1:5000, #MAB374, Millipore) immunoblotting membrane was blocked with 3% non-fat milk in TBS for 1 h at room temperature and incubated overnight at 4^{o}C with primary antibodies diluted in TBS-T. HRP-conjugated antibodies were used for chemiluminescence detection with ECL (GE Healthcare) and protein levels were quantified by densitometry using Image J software and normalized against loading controls HSC70 or GAPDH.

Depletion of Erg expression *in vitro*

To silence Erg expression in either freshly isolated primary MLEC from ECFAK^{Y861F} pups at P6 or PMT FAK^{Y861F}, endothelial cells were seeded in MLEC media without antibiotics at 10^5 cell/six well the day before transfection using 20 nM siRNA against mouse ERG (SMARTpool ON-TARGETplus, #L-040714-01, Dharmacon) - denoted as siRNAERG in the text – and in parallel, 20 nM siRNA an ON-TARGETplus Non-targeting pool was used as negative control siRNA (#D-001810-10, Dharmacon) - denoted as siCtrl. Cell transfection was performed using Oligofectamine reagent (Invitrogen/ThermoFisher Scientific) following the manufacturer's instructions. Gene expression was examined 48h post-transfection, by both qRT-PCR and Western blot analysis as described above.

Mass spectrometry total and phospho-proteomic analysis

Primary mouse lung endothelial cell preparations from ECFAK^{WT} and ECFAK^{KO} pups between P10-P14 were performed as above-described. 10-15 million cells were seeded in 15 cm dishes coated with 0.1% gelatin, 10 μg/ml human plasma fibronectin and 30 μg/ml collagen and incubated for overnight at 37^{o}C and 5% CO_2. Cells were starved with serum-free, unsupplemented media (Opti-MEM I-Gibco, #31985070, ThermoFisher Scientific) for 6 h and stimulated with PBS (control) or VEGF (30 ng/ml) for 30 min. Total cell lysates (2 biological replicates per genotype/condition) were made using SDS solubilization buffer (2% SDS, 100mM Tris-HCl pH7.5) plus 100 mM reducing buffer (DTT). Mass spectrometry sample preparation was carried out utilizing iFASP protocols(McDowell et al., 2013). TMT mass spectormetry runs were performed as described in (Dermit et al., 2020). Mass spectrometry raw data files were searched and quantified by MaxQuant software (Version 1.6.0.16)(Tyanova et al., 2016). The search was performed against Uniprot mouse database (2016) using Andromeda search engine(Tyanova

and Cox, 2018), with a false-discovery rate (FDR) of 0.01. TMT 6plex search type was used, with a reporter mass tolerance of 0.01 Da. Peptide tolerance was set at 20 and 4 ppm for the first search and main search, respectively. The minimum peptide length was set to 7 amino acids. Carbamidomethyl of Cysteine was set as a fixed modification, whereas oxidation of Methionine and protein N-terminal acetylation were set as variable modifications. For phospho-proteomics experiments, Phospho (STY) was included as an additional variable modification. Second peptides and Match between runs were also enabled. All other Maxquant settings were kept as default. Downstream data analysis was then performed with Perseus software (Version 1.6.2.1)((Tyanova and Cox, 2018). Firstly, the data was filtered for 'Potential Contaminant', 'Reverse' and 'Only identified by site' proteins. The data was then log 2 transformed and normalized by median subtraction. A further filtration was performed based on valid values. The FAK^{KO} vs FAK^{WT} ratios were calculated for VEGF treatment and PBS (control) treatment. To identify genes that are significant outliers, Significance A was used with a 5% Benjamini-Hochberg FDR cut-off point. Category annotations were also added to each gene from the following databases: Gene Ontology biological process (GOBP), Gene Ontology cellular component (GOCC), Gene Ontology molecular function (GOMF), Kyoto Encyclopedia of Genes and Genomes (KEGG) names & Uniprot Keywords. Afterwards, category enrichment analysis was performed by 2D annotation enrichment(Tyanova and Cox, 2018), with the threshold set at 2% Benjamini-Hochberg FDR.

All mass spectrometry raw files and their associated MaxQuant output search results were deposited on ProteomeXchange Consortium (Vizcaino et al., 2014) via the PRIDE partner repository (http://www.ebi.ac.uk/pride/archive/), under the accession number PXD030824. All Mass spectrometry raw data files were searched by Maxquant (version 1.6.3.3), using a False discovery Rate (FDR) of <1% for both peptide and protein identifications, calculated

via a reverse database search approach. All downstream statistical analyses were performed by Perseus (version 1.6.2.3). We performed Benjamini-Hochberg FDR calculations for correction of all calculated p-values. For calculation of outliers, an FDR cut-off of <5% was used in a two-way Significance-A test. For annotation enrichment analysis, a Benjamini-Hochberg FDR cut-off of < 2% applied in the adapted Wilcoxon Mann-Whitney test.

Cell fractionations

Primary mouse lung endothelial cell preparations from ECFAK^{WT}, ECFAK^{KO}, ECFAK^{KIWT}, ECFAK^{KD}, ECFAK^{Y397F} and ECFAK^{Y861F} pups at P6 were performed as above-described. 5 million cells were seeded in 10 cm dishes coated with 0.1% gelatin, 10 μg/ml human plasma fibronectin and 30 μg/ml collagen and incubated for overnight at 37^{o}C and 5% CO_2. Cells were starved with serum-free, unsupplemented media (Opti-MEM I-Gibco, #31985070, ThermoFisher Scientific) for 6 h and stimulated with PBS (control) or VEGF (30 ng/ml) for 30 min. After, cells were washed in cold PBS, and lysed with Cyt Buffer (10 mM Tris pH 7.5, 0.05% NP-40, 3 mM $MgCl_2$, 100 mM NaCl, 1 mM EGTA containing PhosStop and cOmplete ULTRA Tablets phosphatases and protease inhibitors (Roche). Cells were scrape-loaded into tubes, incubated for 5 min at 4°C, spun at 800 x g at 4°C (5 min), and cytosolic supernatants collected. Cells pellets were further washed with Cyto buffer twice to remove residual cytosolic proteins. Purified nuclei were resuspended in RIPA buffer, spun at 16,000 x g for 15 min, and the supernatant collected as the nuclear fraction. Alternatively, cytoplasmic and nuclear fractions were separated by using NE-PER Nuclear and Cytoplasmic Extraction Reagents (Thermo Scientific) following manufacturer's instructions. Western blotting was performed on SDS-PAGE gels. Blots were probed utilizing the following antibodies: anti-FAK [clone 4.47] (#05-537, Sigma Aldrich), pY397-FAK (1:1000, #3283,

CST), Lamin A/C [LMNA] (4C11, #MAB4777, CST) and GAPDH (1:5000, #MAB374, Millipore).

Method for Rapid Immunoprecipitation Mass spectrometry of Endogenous proteins

The protocol was adapted from(Mohammed et al., 2016). Briefly, HUVECs (#C2517AS [single donor] Lonza) were grown in complete media (#C-22111, Promocell). Confluent cell cultures ($\sim 10 \times 10^7$ per biological replicate) were starved with serum-free, unsupplemented media (Opti-MEM I-Gibco, ThermoFisher Scientific #31985070) for 6 h and stimulated with PBS (control) or VEGF (50 ng/ml) for 30 min. The media was replaced with Opti-MEM I-Gibco containing 1% formaldehyde (#28908, ThermoFisher Scientific) and crosslinked for 8 min. Crosslinking was quenched by adding glycine to a final concentration of 0.2 M. For the performance of RIME experiments, 15 µl of agarose-conjugated FAK antibody (#16-173, Millipore/MERK) or 15 µg agarose-conjugated mouse IgG or Protein G agarose beads (#sc-2343, Santa Cruz and #A0919, Sigma). For nuclear extraction the cell pellet was resuspended in LB1 buffer (50 mM HEPES-KOH (pH 7.5), 140 mM NaCl, 1 mM EDTA, 10% glycerol, 0.5% NP-40 and 0.25% Triton X-100) followed by rotation mixing for 10 min at 4 °C. Then, nuclei were pelleted and resuspended in LB2 buffer (10 mM Tris-HCL (pH 8.0), 200 mM NaCl, 1 mM EDTA and 0.5 mM EGTA) and rotated at 4 °C for 5 min. The samples were resuspended in LB3 buffer (10 mM Tris-HCl (pH 8), 100 mM NaCl, 1 mM EDTA, 0.5 mM EGTA, 0.1% Na-deoxycholate and 0.5% N-lauroylsarcosine). Chromatin/protein were sheared by sonication (Diagenode) for 10 x 30 sec with 30 sec of rest on ice in between to produce DNA fragments of 100–1,000 bp. The bead-bound antibody and chromatin/protein (300 µg total protein lysates) were incubated overnight at 4^{o}C. The next day the beads were washed 10 times with 1 ml ice-cold RIPA buffer and twice with 500 µl 100 mM AMBIC

(ammonium bicarbonate). The FAK nuclear protein complexes were subjected to on-bead proteolytic digestion, desalting, and liquid chromatography-tandem mass spectrometry, as described (Turriziani et al., 2014) with following alterations. Peptide samples were analysed using a Fusion Lumos mass spectrometer coupled to a RSLC-nano uHPLC pump (both Thermo Fisher) using a 40 minute gradient (2-30% Acetonitrile) over packed emitter (40 cm, 0.075 mm ID) self-packed with 1.9 ReprosilPur AQ (Dr Maisch). The Lumos was operated in OT/IT mode with 120k MS resolution, rapid MS/MS IT and a cycle time of 1s. Mass spectrometry raw data was analysed using MaxQuant 1.5 by searching against the human Uniprot database using standard LFQ parameters, M(Ox) and N-terminal Acetylation as variable modifications, and matching between runs. Differential expression analysis was performed using the Perseus software suite. Transcription factors associated with the mouse ERG promoter, obtained from TRRUST v2 (Transcriptional Regulatory Relationships Unravelled by Sentence-based Text mining, https://www.grnpedia.org)(Han et al., 2018) were used to seed functional protein interaction networks using Qiagen's Ingenuity Pathway Analysis (IPA). Proteins identified using Rapid Immunoprecipitation of Endogenous Proteins (RIME) as FAK interactors under PBS (control) or VEGF-stimulated conditions. Settings used for network generation were; interactions must be upstream of the TF, must be direct and experimentally observed. Analyses were done at $p<0.05$. Final connected networks were exported from IPA and visualized using Cytoscape 3.5.1(Shannon et al., 2003). Data are available via ProteomeXchange with identifier PXD033447.

Competition Migration Assays

Chemotaxis was studied using fluorescent colour dye prelabelled FAK^{WTKI} (green, Cell Tracker Green CMFDA, # C7025, ThermoFisher) and FAK^{WTKI}, FAK^{KD}, FAK^{397F} or FAK^{861F} (red, Cell Tracker Orange CMRA, # C34551, ThermoFisher) primary mouse lung

endothelial cells that were seeded in a ratio of 1:1 in Dunn chambers as in Zicha et al.(Zicha et al., 1997). Briefly, both outer and inner wells were filled with Opti-MEM I-Gibco (#31985070, ThermoFisher Scientific). Cells were grown on glass coverslips overnight followed by serum starvation for at least 3 h in Opti-MEM I. Coverslips were inverted onto the Dunn Chamber and sealed on three sides with hot wax mixture (Vaseline:paraffin=beeswax, 1:1:1). The media was removed from the outer well by capillary action and was rinsed with Opti-MEM I-Gibco before filling with Opti-MEM I containing 30 ng/ml VEGF. The chamber was then sealed with wax and mounted on a fluorescence microscope Zeiss Axio100 inverted microscope equipped with a ×10 objective lens and an environmental chamber that maintained 37 °C and 5% CO_2. Images were acquired taking a frame every 10 min for 24 h using Micromanager (Open source software: https://micro-manager.org). Subsequently, all cells in the acquired time-lapse sequences were tracked using the Ibidi tracking tool in ImageJ (http://rsb.info.nih.gov/ij/plugins/track/track.html).

Competition Sprouting Assays

Fluorescent colour dye prelabelled as above-described, FAK^{WT} (green) vs. FAK^{WT} or FAK^{KO} (red); and FAK^{WTKI} (green) vs. FAK^{WTKI}, FAK^{KD}, FAK^{397F} or FAK^{861F} (red) primary mouse lung endothelial cells were mixed in a ratio of 1:1 (700 cells). Each cell pair set were seeded on the lid of a 15 cm cell culture dish, in MLEC medium supplemented with 0.25% methylcellulose (Sigma), in drops of 20 ul, and left overnight to form the spheroids. The day after, the drops were recovered, centrifuged 150 g no brake, for 5 min, resuspended in collagen 1 mg/ml, and left for 1 h at 37°C and 5% CO_2. Then, EGM2 medium containing VEGF (30ng/ml) was added to each well. Next day, gels were fixed in PFA 4%, and analysed by confocal microscopy imaging (Zeiss LSM LSM710, objective ×20 with NA 0.45, images were acquired using the multi-channel fluorescent in frame mode). The outer cell of each

sprout was identified, and the ratio of red and green tip cells per total sprouts were analysed for each spheroid.

CRISPR/Cas9 genome editing for USP9X and TRIM25

Immortalized MLEC from ECFAK^{WT}, ECFAK^{KO}, ECFAK^{KIWT}, ECFAK^{KD}, ECFAK^{Y397F} and ECFAK^{Y861F} were transfected with murine with the Lenti-CRISPR–EGFP plasmid with inserted gRNAs for murine *Usp9x and Trim25*. The sgRNAs were designed using the CRISPOR algorithm (http://crispor.tefor.net). sgRNA sequences targeting Usp9x (Gene ID: 22284) and Trim25 (Gene ID: 217069) (see Table 2 for targeting sequences) were cloned into the Lenti-CRISPR–EGFP plasmid (Addgene ID: 75159) using BsmBI enzyme site. Mouse Lung Endothelial Cells (MLECs) were plated on cell culture plates coated with 0.1% gelatin, 10 μg/ml human plasma fibronectin and 30 μg/ml collagen and grown in MLEC media, at 37 °C with 5% CO2. Cells were centrifuged at 300 g for 5 min and re-suspended in 100 μL of R1 buffer (Invitrogen) and mixed with CRISPR/Cas9-EGFP plasmid DNA (10 μg) and loaded into a 100 μl Neon electroporation tip (Invitrogen). Electroporations were performed using 1300mV for 20ms with 2 pulse programme on the Neon Electroporator (Invitrogen). After electroporation, cells were left to recover in pre-warmed supplemented MLEC media and further cultured in 6-well plates for 2 days.

The CRISPR/Cas9 knockout cells were enriched by Flow Cytometry. Cells were washed with phosphate-buffered saline (PBS) and harvested with 200 μL of FACS buffer (1% BSA and 0.5 mM EDTA in PBS) 48 h after transfection. A 488-nm diode laser was used for the detection of EGFP. In each sample, viable singlet MLEC cells were gated via forward-scatter (FSC) laser and side-scatter (SSC) and EGFP positive cells, regardless of expression levels, were sorted using a FACS AriaIII flow cytometer (BD Biosciences) at the Chelsea Flow Cytometry and Light Microscopy Facility.

ERG immunoprecipitation

Prior to immunoprecipitation, cells were serum starved in Optimen (Gibco) for 6 h and further stimulated with murine VEGF-A (50 ng/ml; Prepotech) for 30 min. Cells were washed twice with ice cold 1X DPBS and lysed in RIPA buffer (50 mM Tris–HCl, pH7.4, 150 mM NaCl, 1 mM EDTA, 1% NP-40, 1% Sodium Deoxycholic acid, 0.1% SDS) freshly supplemented with protease and phosphatase inhibitors (Cocktail I, II and III; all from Millipore). Lysates were sonicated (15 sec on/off, twice, 50% amplitude), samples were cleared by centrifugation and protein concentration determined by the Bradford procedure (Invitrogen). Equal concentrations of protein extracts were added to Protein G magnetic beads coated (Invitrogen) with anti-ERG antibody (C1, #sc- 376293, Santa Cruz, Santa Cruz Biotechnology) and rotated overnight at 4°C. Protein complexes bound to the beads were collected using a magnetic separator, washed 3 times with washing buffer (Invitrogen), and then eluted by boiling the beads in SDS sample buffer at 95°C for 5 min. Western blotting was performed on SDS-PAGE gels. Blots were probed with an anti-ERG antibody (# ab92513, Abcam). Inputs were analysed by immunoblotting utilizing the following antibodies: anti-USP9X (#A301-351A, Cambridge Bioscience), anti-TRIM25/EFP [EPR7315] (# ab167154, Abcam), anti-ERG [EPR3864] (# ab92513, Abcam), anti-ERG [C1] (#sc- 376293, Santa Cruz, Santa Cruz Biotechnology), anti-FAK [clone 4.47] (#05-537, Sigma Aldrich), and anti-HSC70 (#sc-7298, Santa Cruz).

Ubiquitin Binding Domain proteins assays and Proteasome inhibition.

Prior to Ubiquitin Binding Domain proteins (UBDs) immunoprecipitation, cells were treated with vehicle (DMSO) or MG132 inhibitor (20μg/ml, Millipore) for 4 h. Cells were washed

twice with ice cold 1X DPBS and lysed in Blast lysis buffer (Cytoskeleton Inc). Lysates were cleared by centrifugation and protein concentration determined by the Bradford procedure (Cytoskeleton Inc). Equal concentration of protein extracts was incubated with UBDs coated beads incubated for 2 h at 4°C. Samples were washed three times with washing buffer (Cytoskeleton Inc). Proteins captured by the UBDs were released by denaturation in SDS and analysed by immunoblotting. Antibodies utilized include anti-ERG [EPR3864] (# ab92513, Abcam).

Statistical Analysis

Otherwise indicated, all data are shown as mean ± SE. First, the data was subjected to Rout outlier analysis with a 99% of confident, and then to a D`Agostino-Pearson normality test to analyse the distribution of the data. Parametric and non-parametric test were used depending on the outcome of that analysis. In the case of comparison of two conditions we used t-test analysis. When more than two conditions were present, we used One-Way ANOVA, using Sidak post-test to compare against the control sample. In the case of two groups of two conditions, we proceed with a Two-Way ANOVA using Siddak post-test to compare between groups. All statistical analyses were generated using GraphPad Prism (GraphPad software, version 8) and statistical significance indicated as: $*p < 0.05$, $**p \leq 0.01$, $***p \leq 0.001$, $****p \leq 0.0001$, NS, not significant.

Authors contribution

GD'A designed, executed, analysed and interpreted data for all the experiments including: *in vivo* validation of ECFAK^{KO} and ECFAK^{KI} models (*in vivo* Cre-mediated induction followed fresh analysis of retina and primary lung EC), *in vitro* validation of ECFAK^{KI} model (*in vitro* Cre-mediated induction of immortalized lung ECs), *in vivo* characterization of ECFAK^{KO}

(retinal vascular patterning and molecular [ERG and DLL4] phenotypes) and ECFAK^{KI} (retina patterning and molecular [ERG and DLL4] phenotypes), *in vitro* competitive sprouting (ECFAK^{KO} and ECFAK^{KI} in both primary and immortalized lung EC), *in vitro* competitive migration (in ECFAK^{KI} primary lung ECs), *in vivo* ERG rescue experiments (in ECFAK^{KO} and ECFAK^{KI} mice), *in vitro* experiments for the identification of the endothelial nuclear FAK molecular mechanism (FAK/USP9x/TRIM25/ERG): proteomics (in *in vivo* Cre-mediated depleted and freshly isolated primary lung FAK^{KO} ECs), cellular fractionations (in *in vivo* Cre-mediated depletion/expression and freshly isolated primary lung FAK^{KO} and FAK^{KI} ECs), RIME (in HUVEC), CRISPR/Cas9 (in immortalized lung FAK^{KO} and ECFAK^{KI} ECs). GD'A assisted with establishment of the collaborations, conceptualized and the wrote the paper. IF designed, executed, analysed, and interpreted data for *in vitro* validation of ECFAK^{KI} model (immortalization of lung EC and *in vitro* Cre-mediated induction), *in vivo* characterization of ECFAK^{KO} (retinal vascular patterning and molecular [DLL4] phenotypes) and ECFAK^{KI} (retinal vascular patterning and initiated the molecular [DLL4] phenotypes). JG-E, helped to write the final version of the manuscript; designed and modified figures, performed *in vitro* experiments, cultured cells, performed immunoprecipitation, nuclear fractionations, and western blot from CRISPR-cas9 knockout and Knock-in endothelial cells; completed and examined competitive sprouting (3D) assays; analysed data and performed image and statistical analysis. EM and JW assisted with bioinformatic analysis. HK designed the Usp9x and TRIM25 and assisted with generation of CRISPR-Cas9/knockout cell lines. MSB assisted with execution and analysis of proteomic data. FKM and MSA designed the TMT proteomics experiments and performed the data analysis. BS provided technical expertise for RIME, assisted with RIME analysis and generation of the endothelial nuclear FAK interactome. A. Serrels facilitated the Mass Spectrometry core facility (University of Edinburgh) for RIME analysis and provided

scientific advice in nuclear FAK. MP executed and helped analyse competitive cell migration (2D) assays. GD'A and A. Squire developed the software scripts for quantitation of ERG expression analysis *in vivo*. GMB and AMR provided critical ERG reagents (AdERG virus and pS215ERG antibody), scientific advice and technical expertise. RG and YW helped with the large-scale production of AdLacZ and AdERG viruses. LER assisted with primary EC isolation, help with design of experiments, and performed western blot analysis. NB generated the first generation of immortalized ECs from the knockin mice and assisted IF with the maintenance of the mice. PM provided reagents, tools and facilities (Institute of Cancer Research, London) for generation for Cas9/CRISPR gene editing. KMH-D designed the project, established the collaborations, conceptualized, and co-wrote the paper. All authors read and comment on the manuscript.

Authors contribution

GD'A designed, executed, analysed and interpreted data for all the experiments including: *in vivo* validation of ECFAK^{KO} and ECFAK^{KI} models (*in vivo* Cre-mediated induction followed fresh analysis of retina and primary lung EC), *in vitro* validation of ECFAK^{KI} model (*in vitro* Cre-mediated induction of immortalized lung ECs), *in vivo* characterization of ECFAK^{KO} (retinal vascular patterning and molecular [ERG and DLL4] phenotypes) and ECFAK^{KI} (retina patterning and molecular [ERG and DLL4] phenotypes), *in vitro* competitive sprouting (ECFAK^{KO} and ECFAK^{KI} in both primary and immortalized lung EC), *in vitro* competitive migration (in ECFAK^{KI} primary lung ECs), *in vivo* ERG rescue experiments (in ECFAK^{KO} and ECFAK^{KI} mice), *in vitro* experiments for the identification of the endothelial nuclear FAK molecular mechanism (FAK/USP9x/TRIM25/ERG): proteomics (in *in vivo* Cre-mediated depleted and freshly isolated primary lung FAK^{KO} ECs), cellular fractionations (in *in vivo* Cre-mediated depletion/expression and freshly isolated primary

lung FAK^{KO} and FAK^{KI} ECs), RIME (in HUVEC), CRISPR/Cas9 (in immortalized lung FAK^{KO} and ECFAK^{KI} ECs). GD'A assisted with establishment of the collaborations, conceptualized and the wrote the paper. IF designed, executed, analysed and interpreted data for *in vitro* validation of ECFAK^{KI} model (immortalization of lung EC and *in vitro* Cre-mediated induction), *in vivo* characterization of ECFAK^{KO} (retinal vascular patterning and molecular [DLL4] phenotypes) and ECFAK^{KI} (retinal vascular patterning and initiated the molecular [DLL4] phenotypes). JG-E, helped to write the final version of the manuscript; designed and modified figures, performed *in vitro* experiments, cultured cells, performed immunoprecipitation, nuclear fractionations, and western blot from CRISPR-cas9 knockout and Knock-in endothelial cells; completed and examined competitive sprouting (3D) assays; analysed data and performed image and statistical analysis. EM and JW assisted with bioinformatic analysis. HK designed the Usp9x and TRIM25 and assisted with generation of CRISPR-Cas9/knockout cell lines. MSB assisted with execution and analysis of proteomic data. FKM and MSA designed the TMT proteomics experiments and performed the data analysis. BS provided technical expertise for RIME, assisted with RIME analysis and generation of the endothelial nuclear FAK interactome. A.B-C Did the sample processing, LC-MS/MS, Data search and bioinformatic analysis to determine specific/regulated FAK interactions for RIME analysis; A. Serrels facilitated the Mass Spectrometry core facility (University of Edinburgh) for RIME analysis and provided scientific advice in nuclear FAK. MP executed and helped analyse competitive cell migration (2D) assays. GD'A and A. Squire developed the software scripts for quantitation of ERG expression analysis *in vivo*. GMB and AMR provided critical ERG reagents (AdERG virus and pS215ERG antibody), scientific advice and technical expertise. RG and YW helped with the large-scale production of AdLacZ and AdERG viruses. LER assisted with primary EC isolation, help with design of experiments, and performed western blot analysis. NB generated the first generation of

immortalized ECs from the knockin mice and assisted IF with the maintenance of the mice. PM provided reagents, tools and facilities (Institute of Cancer Research, London) for generation for Cas9/CRISPR gene editing. KMH-D designed the project, established the collaborations, conceptualized and co-wrote the paper. All authors read and comment on the manuscript.

Acknowledgments

We thank Julie Holdsworth and Bruce Williams for mouse technical assistance. Billie Griffith for help with the RIME protocol and Alex von Kriegsheim (Mass spectrometry facilities manager, Edinburgh Cancer Research Centre) for his help in providing the technical details of the RIME work and uploading data to ProteomeXchange; Annika N. Alexopoulou, Delphine M. Lees, Vassiliki Kostourou, Silvia Batista and Bernardo Tavora for the development of the first generations of FAK-knockin mutant mice and ECs; Pedro Cutillas and Vinothini Rajeeve for facilitating the Mass Spectrometry for the phospho-proteomic analysis (Barts Cancer Institute, London).

Competing interests

The authors declare no competing financial interests, except for KHD is a scientific advisor for Ellipses and is a joint applicant on patent claims N421127GB and N417173GB.

Funding

GD'A was funded by Barts Charity (472/2174). IF, NB, JG-E were funded by Cancer Research UK (A18673). HK and PM were funded by (Breast Cancer Now as part of Programme Funding to the Breast Cancer Now Toby Robins Research Centre (CTR-QR14-007). We acknowledge NHS funding to the NIHR Biomedical Research Centre. EM, and JW

are supported by (CRUK-Barts Cancer centre funds). LR was supported by MRC funds MR/V009621/1 and Cancer Research UK (A18673). MSA and FKM are funded and supported by a Medical Research Council Career Development Award (MR/P009417/1) and a Barts Charity grant (MGU0346) to FKM, and a Barry Read PhD studentship to MSA. RG and YW were supported by CRUK grant: A27224. KH-D is HEFCE funded and has had a Cancer Research UK programme grant (C82181/A12007) and recently (DRCNPG-May21\100004) which now supports LR. The laboratory was also supported by funds from Barts Charity (MGU0487) and the CRUK City of London Major Centre. AB-C Wellcome Trust (Multiuser Equipment 208402/Z/17). A Serrels, Cancer Research UK (grant number C39669/A25919). A Squire employed by the University Clinic Essen. B Serrels was HEFCE supported. GMB, British Heart Foundation Project Grant PG/17/33/32990. AMR, British Heart Foundation Programme Grant RG/17/4/32662.

Data and materials availability

The FAK knockin mice are available from KMH-D under a material agreement with the BCI, QMUL. The phospho-proteomics and RIME proteomics data have been deposited to the ProteomeXchange Consortium via the PRIDE partner repository under accession number PXD030824.

References

ABU-GHAZALEH, R., KABIR, J., JIA, H., LOBO, M. & ZACHARY, I. 2001. Src mediates stimulation by vascular endothelial growth factor of the phosphorylation of focal adhesion kinase at tyrosine 861, and migration and anti-apoptosis in endothelial cells. *Biochem J,* 360**,** 255-64.

ALEXOPOULOU, A. N., LEES, D. M., BODRUG, N., LECHERTIER, T., FERNANDEZ, I., D'AMICO, G., DUKINFIELD, M., BATISTA, S., TAVORA, B., SERRELS, B. & HODIVALA-DILKE, K. 2017. Focal Adhesion Kinase (FAK) tyrosine 397E mutation restores the vascular leakage defect in endothelium-specific FAK-kinase dead mice. *J Pathol,* 242**,** 358-370.

BAUTCH, V. L. 2012. VEGF-directed blood vessel patterning: from cells to organism. *Cold Spring Harb Perspect Med,* 2**,** a006452.

BIRDSEY, G. M., SHAH, A. V., DUFTON, N., REYNOLDS, L. E., OSUNA ALMAGRO, L., YANG, Y., ASPALTER, I. M., KHAN, S. T., MASON, J. C., DEJANA, E., GOTTGENS, B., HODIVALA-DILKE, K., GERHARDT, H., ADAMS, R. H. & RANDI, A. M. 2015. The endothelial transcription factor ERG promotes vascular stability and growth through Wnt/beta-catenin signaling. *Dev Cell,* 32**,** 82-96.

BLANCO, R. & GERHARDT, H. 2013. VEGF and Notch in tip and stalk cell selection. *Cold Spring Harb Perspect Med,* 3**,** a006569.

BRAREN, R., HU, H., KIM, Y. H., BEGGS, H. E., REICHARDT, L. F. & WANG, R. 2006. Endothelial FAK is essential for vascular network stability, cell survival, and lamellipodial formation. *J Cell Biol,* 172**,** 151-62.

CAI, H., FIELDS, M. A., HOSHINO, R. & PRIORE, L. V. 2012. Effects of aging and anatomic location on gene expression in human retina. *Front Aging Neurosci,* 4**,** 8.

CLAXTON, S., KOSTOUROU, V., JADEJA, S., CHAMBON, P., HODIVALA-DILKE, K. & FRUTTIGER, M. 2008. Efficient, inducible Cre-recombinase activation in vascular endothelium. *Genesis,* 46**,** 74-80.

CORSI, J. M., HOUBRON, C., BILLUART, P., BRUNET, I., BOUVREE, K., EICHMANN, A., GIRAULT, J. A. & ENSLEN, H. 2009. Autophosphorylation-independent and -dependent functions of focal adhesion kinase during development. *J Biol Chem,* 284**,** 34769-76.

DERMIT, M., DODEL, M., LEE, F. C. Y., AZMAN, M. S., SCHWENZER, H., JONES, J. L., BLAGDEN, S. P., ULE, J., & MARDAKHEH, F. K. 2020. Subcellular mRNA Localization Regulates Ribosome Biogenesis in Migrating Cells. Developmental Cell. 55(3): 298–313.e10

DUFTON, N. P., PEGHAIRE, C. R., OSUNA-ALMAGRO, L., RAIMONDI, C., KALNA, V., CHUAHAN, A., WEBB, G., YANG, Y., BIRDSEY, G. M., LALOR, P., MASON, J. C., ADAMS, D. H., & RANDI, A. M. 2017. Dynamic regulation of canonical TGFβ signalling by endothelial transcription factor ERG protects from liver fibrogenesis. Nature Communications. 8: 895

FAINGOLD, D., FILHO, V. B., FERNANDES, B., JAGAN, L., DE BARROS, A. M., JR., ORELLANA, M. E., ANTECKA, E. & BURNIER, M. N., JR. 2014. Expression of focal adhesion kinase in uveal melanoma and the effects of Hsp90 inhibition by 17-AAG. *Pathol Res Pract,* 210**,** 739-45.

FISH, J. E., CANTU GUTIERREZ, M., DANG, L. T., KHYZHA, N., CHEN, Z., VEITCH, S., CHENG, H. S., KHOR, M., ANTOUNIANS, L., NJOCK, M. S., BOUDREAU, E., HERMAN, A. M., RHYNER, A. M., RUIZ, O. E., EISENHOFFER, G. T., MEDINA-RIVERA, A., WILSON, M. D. & WYTHE, J. D. 2017. Dynamic regulation of VEGF-inducible genes by an ERK/ERG/p300 transcriptional network. *Development,* 144**,** 2428-2444.

FRANCO, C. A., JONES, M. L., BERNABEU, M. O., GEUDENS, I., MATHIVET, T., ROSA, A., LOPES, F. M., LIMA, A. P., RAGAB, A., COLLINS, R. T., PHNG, L. K., COVENEY, P. V. & GERHARDT, H. 2015. Dynamic endothelial cell rearrangements drive developmental vessel regression. *PLoS Biol,* 13**,** e1002125.

GAN, W., DAI, X., LUNARDI, A., LI, Z., INUZUKA, H., LIU, P., VARMEH, S., ZHANG, J., CHENG, L., SUN, Y., ASARA, J. M., BECK, A. H., HUANG, J., PANDOLFI, P. P. & WEI, W. 2015. SPOP Promotes Ubiquitination and Degradation of the ERG Oncoprotein to Suppress Prostate Cancer Progression. *Mol Cell,* 59**,** 917-30.

GIERISCH, M. E., PFISTNER, F., LOPEZ-GARCIA, L. A., HARDER, L., SCHAFER, B. W. & NIGGLI, F. K. 2016. Proteasomal Degradation of the EWS-FLI1 Fusion Protein Is Regulated by a Single Lysine Residue. *J Biol Chem,* 291**,** 26922-26933.

GUPTA, S., ILJIN, K., SARA, H., MPINDI, J. P., MIRTTI, T., VAINIO, P., RANTALA, J., ALANEN, K., NEES, M. & KALLIONIEMI, O. 2010. FZD4 as a mediator of ERG oncogene-induced WNT signaling and epithelial-to-mesenchymal transition in human prostate cancer cells. *Cancer Res,* 70**,** 6735-45.

HAN, H., CHO, J. W., LEE, S., YUN, A., KIM, H., BAE, D., YANG, S., KIM, C. Y., LEE, M., KIM, E., LEE, S., KANG, B., JEONG, D., KIM, Y., JEON, H. N., JUNG, H., NAM, S., CHUNG, M., KIM, J. H. & LEE, I. 2018. TRRUST v2: an expanded reference database of human and mouse transcriptional regulatory interactions. *Nucleic Acids Res,* 46**,** D380-D386.

JAKOBSSON, L., FRANCO, C. A., BENTLEY, K., COLLINS, R. T., PONSIOEN, B., ASPALTER, I. M., ROSEWELL, I., BUSSE, M., THURSTON, G., MEDVINSKY, A., SCHULTE-MERKER, S. & GERHARDT, H. 2010. Endothelial cells dynamically compete for the tip cell position during angiogenic sprouting. *Nat Cell Biol,* 12**,** 943-53.

JUNGE, H. J., YANG, S., BURTON, J. B., PAES, K., SHU, X., FRENCH, D. M., COSTA, M., RICE, D. S. & YE, W. 2009. TSPAN12 regulates retinal vascular development by promoting Norrin- but not Wnt-induced FZD4/beta-catenin signaling. *Cell,* 139**,** 299-311.

KLOSE, R., BERGER, C., MOLL, I., ADAM, M. G., SCHWARZ, F., MOHR, K., AUGUSTIN, H. G. & FISCHER, A. 2015. Soluble Notch ligand and receptor peptides act antagonistically during angiogenesis. *Cardiovasc Res,* 107**,** 153-63.

LIM, S. T. 2013. Nuclear FAK: a new mode of gene regulation from cellular adhesions. *Mol Cells,* 36**,** 1-6.

LIM, S. T., CHEN, X. L., TOMAR, A., MILLER, N. L., YOO, J. & SCHLAEPFER, D. D. 2010. Knock-in mutation reveals an essential role for focal adhesion kinase activity in blood vessel morphogenesis and cell motility-polarity but not cell proliferation. *J Biol Chem,* 285**,** 21526-36.

LOBOV, I. B., RENARD, R. A., PAPADOPOULOS, N., GALE, N. W., THURSTON, G., YANCOPOULOS, G. D. & WIEGAND, S. J. 2007. Delta-like ligand 4 (Dll4) is induced by VEGF as a negative regulator of angiogenic sprouting. *Proc Natl Acad Sci U S A,* 104**,** 3219-24.

LOONEY, A. P., HAN, R., STAWSKI, L., MARDEN, G., IWAMOTO, M., & TROJANOWSKA, M. 2017. Synergistic role of endothelial erg and fli1 in mediating pulmonary vascular homeostasis. *American Journal of Respiratory Cell and Molecular Biology*. 57(1): 121–131

MCDOWELL, G. S., GAUN, A. & STEEN, H. 2013. iFASP: combining isobaric mass tagging with filter-aided sample preparation. *J Proteome Res,* 12**,** 3809-12.

MITRA, S. K., HANSON, D. A. & SCHLAEPFER, D. D. 2005. Focal adhesion kinase: in command and control of cell motility. *Nat Rev Mol Cell Biol,* 6**,** 56-68.

MOHAMMED, H., TAYLOR, C., BROWN, G. D., PAPACHRISTOU, E. K., CARROLL, J. S. & D'SANTOS, C. S. 2016. Rapid immunoprecipitation mass spectrometry of endogenous proteins (RIME) for analysis of chromatin complexes. *Nat Protoc,* 11**,** 316-26.

NEWPORT, E., PEDROSA, A. R., LEES, D., DUKINFIELD, M., CARTER, E., GOMEZ-ESCUDERO, J., CASADO, P., RAJEEVE, V., REYNOLDS, L. E., CUTILLAS, P., DUFFY, S. W., DELGADO, B. L. & HODIVALA-DILKE, K. 2022. Elucidating the role of the kinase activity of endothelial cell focal adhesion kinase in angiocrine signalling and tumour growth. *J Pathol*. 2022 Feb;256(2):235-247.

PEDROSA, A. R., BODRUG, N., GOMEZ-ESCUDERO, J., CARTER, E. P., REYNOLDS, L. E., GEORGIOU, P. N., FERNANDEZ, I., LEES, D. M., KOSTOUROU, V., ALEXOPOULOU, A. N., BATISTA, S., TAVORA, B., SERRELS, B., PARSONS, M., ISKRATSCH, T. & HODIVALA-DILKE, K. M. 2019. Tumor Angiogenesis Is Differentially Regulated by Phosphorylation of Endothelial Cell Focal Adhesion Kinase Tyrosines-397 and -861. *Cancer Res,* 79**,** 4371-4386.

PITULESCU, M. E., SCHMIDT, I., BENEDITO, R. & ADAMS, R. H. 2010. Inducible gene targeting in the neonatal vasculature and analysis of retinal angiogenesis in mice. *Nat Protoc,* 5**,** 1518-34.

REYNOLDS, L. E. & HODIVALA-DILKE, K. M. 2006. Primary mouse endothelial cell culture for assays of angiogenesis. *Methods Mol Med,* 120**,** 503-9.

SCHALLER, M. D. 2010. Cellular functions of FAK kinases: insight into molecular mechanisms and novel functions. *J Cell Sci,* 123**,** 1007-13.

SHAH, A. V., BIRDSEY, G. M., PEGHAIRE, C., PITULESCU, M. E., DUFTON, N. P., YANG, Y., WEINBERG, I., OSUNA ALMAGRO, L., PAYNE, L., MASON, J. C., GERHARDT, H., ADAMS, R. H. & RANDI, A. M. 2017. The endothelial transcription factor ERG mediates Angiopoietin-1-dependent control of Notch signalling and vascular stability. *Nat Commun,* 8**,** 16002.

SHAH, A. V., BIRDSEY, G. M. & RANDI, A. M. 2016. Regulation of endothelial homeostasis, vascular development and angiogenesis by the transcription factor ERG. *Vascul Pharmacol,* 86**,** 3-13.

SHANNON, P., MARKIEL, A., OZIER, O., BALIGA, N. S., WANG, J. T., RAMAGE, D., AMIN, N., SCHWIKOWSKI, B. & IDEKER, T. 2003. Cytoscape: a software environment for integrated models of biomolecular interaction networks. *Genome Res,* 13**,** 2498-504.

SHEN, T. L., PARK, A. Y., ALCARAZ, A., PENG, X., JANG, I., KONI, P., FLAVELL, R. A., GU, H. & GUAN, J. L. 2005. Conditional knockout of focal adhesion kinase in endothelial cells reveals its role in angiogenesis and vascular development in late embryogenesis. *J Cell Biol,* 169**,** 941-52.

SPERONE, A., DRYDEN, N. H., BIRDSEY, G. M., MADDEN, L., JOHNS, M., EVANS, P. C., MASON, J. C., HASKARD, D. O., BOYLE, J. J., PALEOLOG, E. M. & RANDI, A. M. 2011. The transcription factor Erg inhibits vascular inflammation by repressing NF-kappaB activation and proinflammatory gene expression in endothelial cells. *Arterioscler Thromb Vasc Biol,* 31**,** 142-50.

TAVORA, B., BATISTA, S., ALEXOPOULOU, A. N., KOSTOUROU, V., FERNANDEZ, I., ROBINSON, S. D., LEES, D. M., SERRELS, B. & HODIVALA-DILKE, K. 2014. Generation of point-mutant FAK knockin mice. *Genesis,* 52**,** 907-15.

TAVORA, B., BATISTA, S., REYNOLDS, L. E., JADEJA, S., ROBINSON, S., KOSTOUROU, V., HART, I., FRUTTIGER, M., PARSONS, M. & HODIVALA-DILKE, K. M. 2010. Endothelial FAK is required for tumour angiogenesis. *EMBO Mol Med,* 2**,** 516-28.

TURRIZIANI, B., GARCIA-MUNOZ, A., PILKINGTON, R., RASO, C., KOLCH, W. & VON KRIEGSHEIM, A. 2014. On-beads digestion in conjunction with data-dependent mass spectrometry: a shortcut to quantitative and dynamic interaction proteomics. *Biology (Basel),* 3**,** 320-32.

TYANOVA, S. & COX, J. 2018. Perseus: A Bioinformatics Platform for Integrative Analysis of Proteomics Data in Cancer Research. *Methods Mol Biol,* 1711**,** 133-148.

TYANOVA, S., TEMU, T. & COX, J. 2016. The MaxQuant computational platform for mass spectrometry-based shotgun proteomics. *Nat Protoc,* 11**,** 2301-2319.

UBEZIO, B., BLANCO, R. A., GEUDENS, I., STANCHI, F., MATHIVET, T., JONES, M. L., RAGAB, A., BENTLEY, K. & GERHARDT, H. 2016. Synchronization of endothelial Dll4-Notch dynamics switch blood vessels from branching to expansion. *Elife,* 5.

WANG, S., KOLLIPARA, R. K., HUMPHRIES, C. G., MA, S. H., HUTCHINSON, R., LI, R., SIDDIQUI, J., TOMLINS, S. A., RAJ, G. V. & KITTLER, R. 2016. The ubiquitin ligase TRIM25 targets ERG for degradation in prostate cancer. *Oncotarget,* 7**,** 64921-64931.

WANG, S., KOLLIPARA, R. K., SRIVASTAVA, N., LI, R., RAVINDRANATHAN, P., HERNANDEZ, E., FREEMAN, E., HUMPHRIES, C. G., KAPUR, P., LOTAN, Y., FAZLI, L., GLEAVE, M. E., PLYMATE, S. R., RAJ, G. V., HSIEH, J. T. & KITTLER, R. 2014. Ablation of the oncogenic transcription factor ERG by deubiquitinase inhibition in prostate cancer. *Proc Natl Acad Sci U S A,* 111**,** 4251-6.

WANG, Y., HALLDEN, G., HILL, R., ANAND, A., LIU, T. C., FRANCIS, J., BROOKS, G., LEMOINE, N. & KIRN, D. 2003. E3 gene manipulations affect oncolytic adenovirus activity in immunocompetent tumor models. *Nat Biotechnol,* 21**,** 1328-35.

WYTHE, J. D., DANG, L. T., DEVINE, W. P., BOUDREAU, E., ARTAP, S. T., HE, D., SCHACHTERLE, W., STAINIER, D. Y., OETTGEN, P., BLACK, B. L., BRUNEAU, B. G. & FISH, J. E. 2013. ETS factors regulate Vegf-dependent arterial specification. *Dev Cell,* 26**,** 45-58.

ZHAO, X., PENG, X., SUN, S., PARK, A. Y. & GUAN, J. L. 2010. Role of kinase-independent and -dependent functions of FAK in endothelial cell survival and barrier function during embryonic development. *J Cell Biol,* 189**,** 955-65.

ZICHA, D., DUNN, G. & JONES, G. 1997. Analyzing chemotaxis using the Dunn direct-viewing chamber. *Methods Mol Biol,* 75**,** 449-57.

Figures

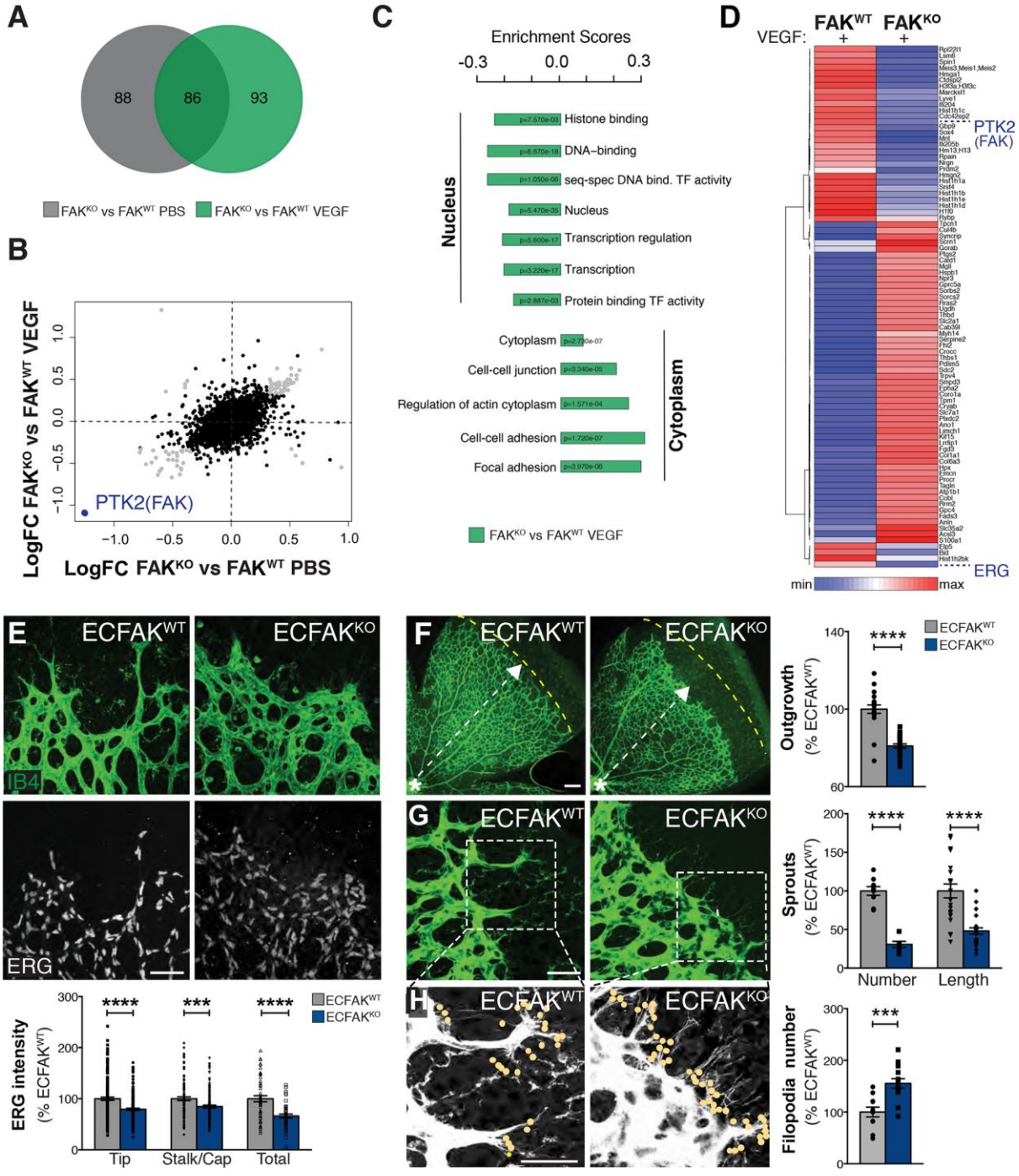

Fig. 1. ERG transcription factor expression is decreased in the absence of endothelial-cell FAK. (**A**) Venn diagram depicting differentially expressed (DE) peptides (p<0.05, Benjamini-Hochberg test) from Liquid chromatography-tandem mass spectrometry (phospho)proteomic analysis of FAK^{WT} and FAK^{KO} primary endothelial cells. (**B**) Scatterplot of logFC of all detected proteins, confirming the knockdown of PTK2 (FAK). (**C**) Bar chart showing protein category enrichment analysis of FAK^{KO} vs FAK^{WT} ECs, after VEGF treatment. Selected GOBP, GOCC, GOMF, KEGG and Uniprot Keywords terms are displayed with Benjamini-Hochberg corrected p-values. (**D**) Hierarchical clustering heatmap of common DE 86 proteins. Each column is the mean of the log2 normalized values from each biological replicate (n=2) for FAK^{WT} and FAK^{KO} genotypes in VEGF condition. (**E**) Representative confocal images of ERG/IB4 doubled-stained and immunofluorescence quantitation of nuclear ERG levels in Tip, Stalk/Cap (capillary) and Total ECs in P6 $ECFAK^{WT}$ and $ECFAK^{KO}$ retinal angiogenic fronts. Bar chart quantitation of ERG levels in $ECFAK^{WT}$ and $ECFAK^{KO}$ retina vasculature. (**F**) Vascular outgrowth. *Dashed line*: mean angiogenic front distance in P6 $ECFAK^{WT}$. *Asterisk*: optic stalk. *Arrow*: vascular outgrowth. (**G**) Sprout numbers and length. (**H**) Filopodia numbers (*dots*, filopodia extensions). Bars, mean + SE for n:4-6 mice per genotype. Student t-test was used for panels E-H. ***p<0.001; ****p<0.0001. Scale bars: 50 μm.

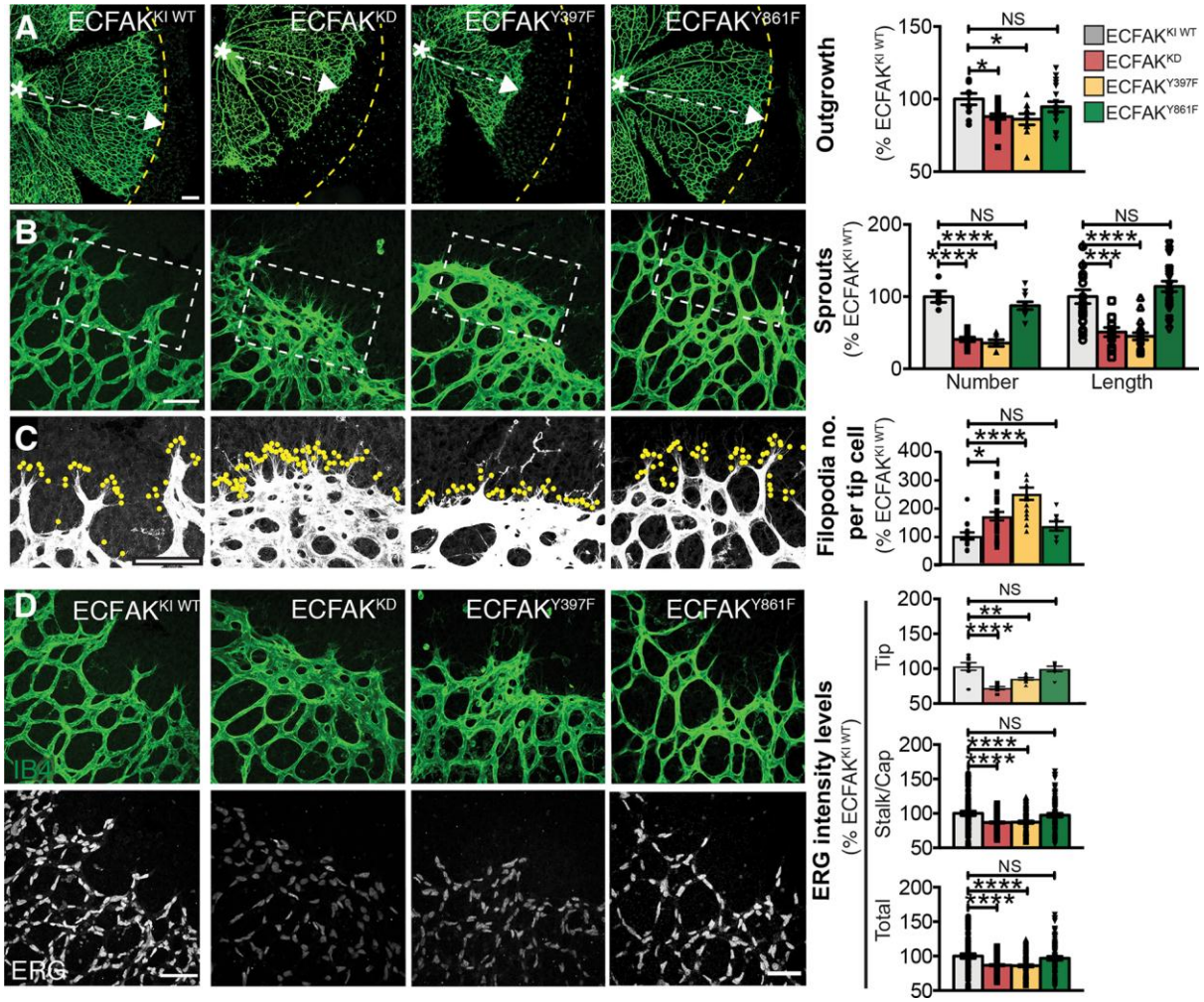

Fig. 2. ERG levels and vascular patterning are reduced by impaired endothelial-cell FAK-kinase activity and non-phosphorylation at Y397. (**A**) Representative confocal images of IB4-stained P6 ECFAK^{WTKI}; ECFAK^{KD}; ECFAK^{Y397F}; and ECFAK^{Y861F} retinal angiogenic fronts with outgrowth quantitation. *Dashed line*: mean angiogenic front distance in P6 ECFAK^{WTKI}. *Asterisk*: optic stalk. *Arrow*: vascular outgrowth. (**B**) Examination of vascular sprout numbers and length; and (**C**) Filopodia numbers (*dots*, filopodia extensions). (**D**) ERG/IB4 doubled-immunofluorescence images in ECFAK^{WTKI}; ECFAK^{KD}; ECFAK^{Y397F}; and ECFAK^{Y861F} retinal vasculature with quantitation of nuclear ERG protein levels in Tip, Stalk/Cap (capillary) and Total ECs in P6 ECFAK mutant retinal angiogenic fronts. Bars, mean + SE for *n*:3-6 mice per genotype. One-Way ANOVA was used in all panels. *p<0.05; **p<0.01; ***p<0.001; ****p<0.0001; NS, not significant. Scale bars: 50 μm

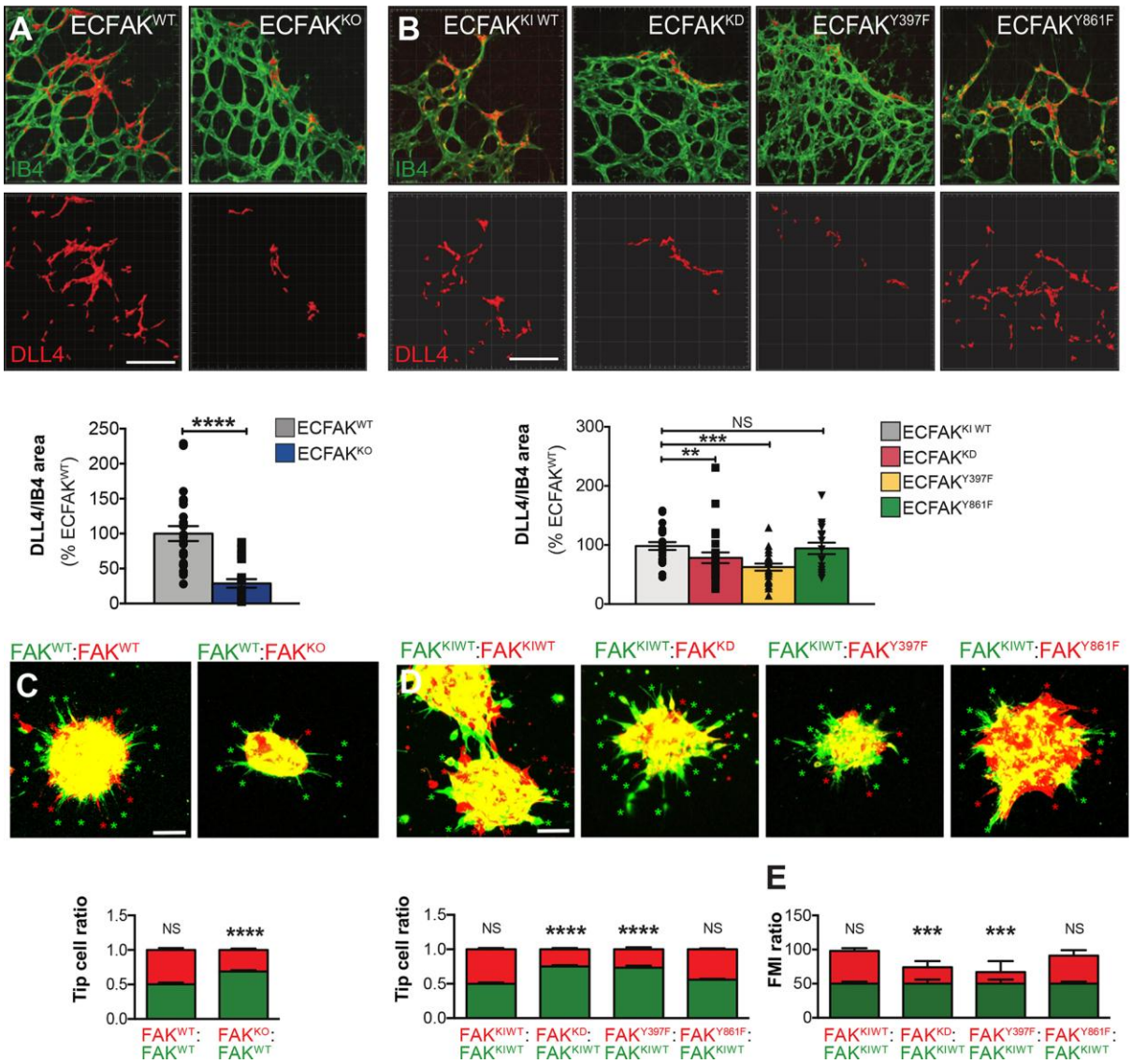

Fig. 3. DLL4 expression and tip cell positioning are associated with endothelial-cell FAK-deficiency, FAK-kinase activity and phosphorylation at FAK-Y397. IMARIS 3D visualization of DLL4/IB4 double-stained P6 retinal angiogenic fronts and DLL4 quantitation *in vivo* in: (**A**) ECFAK^{WT} and ECFAK^{KO} and (**B**) ECFAK^{KIWT}, ECFAK^{KD}, ECFAK^{Y397F} and ECFAK^{Y861F} mice. *n*:4-6 mice for A; 3-6 mice for B. Student t-test was used in A, One-Way ANOVA in B. (**C**) FAK^{WT} and FAK^{KO} or (**D**) FAK^{KIWT}, FAK^{KD}, FAK^{Y397F} and FAK^{Y861F} mutant EC lines, confocal images and quantitation of *in vitro* sprouting competition assays of differentially labelled (green- or red-dye). *Asterisks*, endothelial cell at the tip position.

n: 10-20 spheroids per condition from 2 independent experiments. Two-Way ANOVA was used. (**E**) VEGF-induced migration competition assays *in vitro* between FAK^{KIWT} (green) and FAK^{KIWT}, FAK^{KD}, FAK^{397F} or FAK^{861F} (red) primary mouse lung ECs. Forward Migration Index (FMI) quantitations are shown. *n:* 3 independent experiments analysing 31-60 cells per condition in each of them. Two-Way ANOVA was used. Bars, mean + SE; **p*<0.05; ***p*<0.01; ****p*<0.001; *****p*<0.0001; NS, not significant. Scale bars: 50 μm.

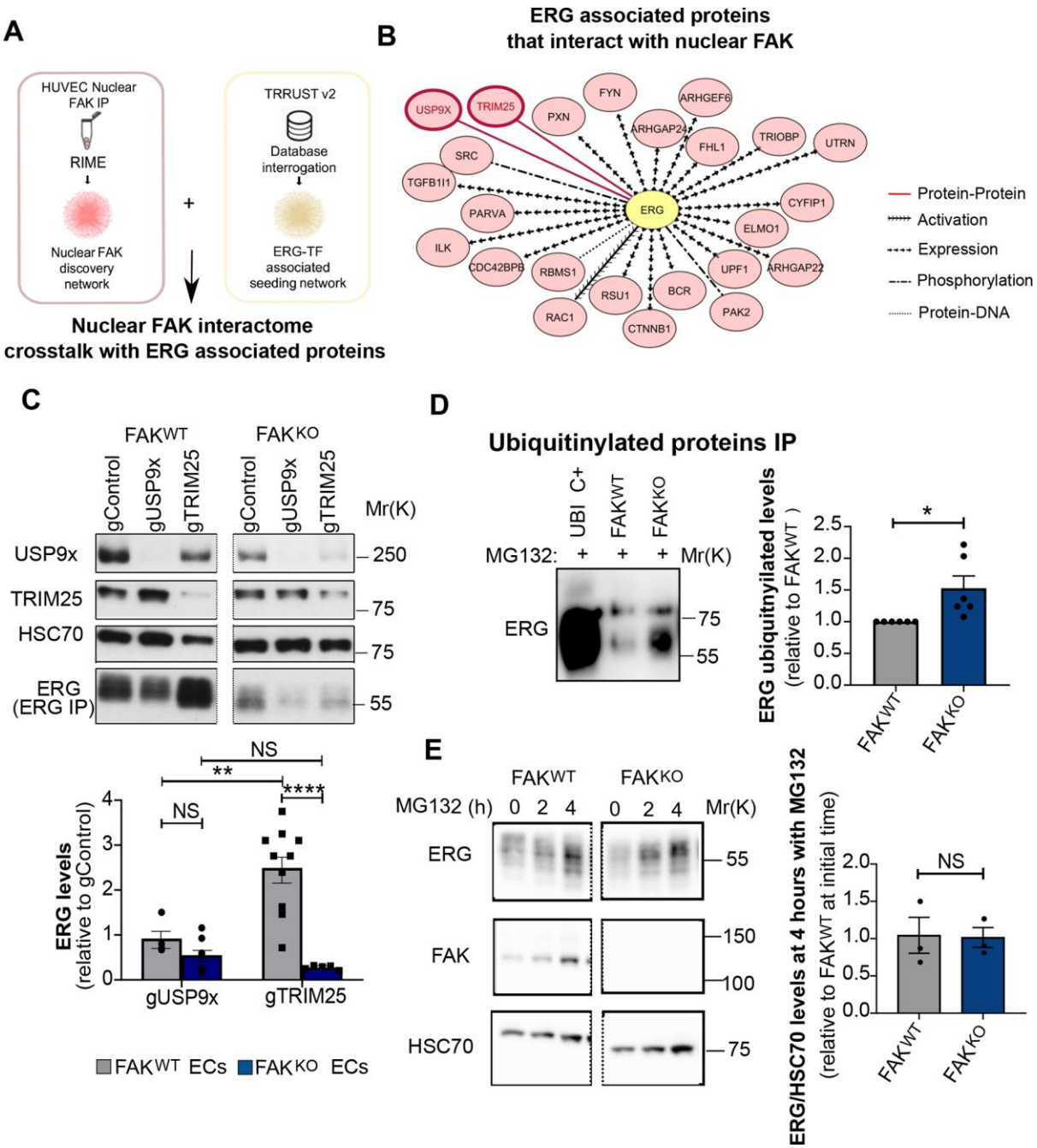

Fig 4. Nuclear ECFAK interacts with USP9x and TRIM25 to regulate ERG levels. (**A**) Interactome network overlapping of nuclear endothelial-cell FAK interactome (RIME) with ERG-associated transcription factors (TRRUST v2). *n:* 25 biological replicates (**B**) Molecules associated with ERG were used to seed a functional interaction network (Qiagen's Ingenuity Pathway Analysis) with nuclear FAK interactors under PBS control and nuclear FAK interactions under VEGF stimulated conditions. Legend, interaction type. Direction of

arrowhead denotes direction of association. Settings used for network generation where interactions must be experimentally observed upstream or downstream of the TF, interactions must be direct. Benjamini-Hochberg test was used selecting interactors with $p<0.05$. **(C)** Western blot analysis of USP9x and TRIM25 in gControl, gUSP9X and gTRIM25 CRISPR/Cas9-depleted FAK^{WT} and FAK^{KO} ECs. Lower panel shows ERG IP followed by ERG western blot. Images of the immunoblots shown were cropped and correspond to the same membrane and exposure. Bar charts, ERG levels relative to gControl for each genotype. *n:* 3-10 replicates from 3-5 independent experiments. Two-Way ANOVA was used. (**D**) Immunoprecipitation for ubiquitinylated proteins followed by western blotting for ERG in FAK^{WT} and FAK^{KO} ECs treated with MG132 proteasome inhibitor for 4 hours. *n:* 6 independent experiments. Wilcoxon rank test was used. (**E**) Western blot analysis for ERG and FAK in FAK^{WT} and FAK^{KO} ECs treated with MG132 for 0, 2 and 4 hours. Images of the immunoblots shown were cropped and correspond to the same membrane and exposure. Quantification of ERG/HSC70 level ratios at 4 hours after MG132 treatment compared to FAK^{WT} ECs at time zero. *n:* 3 independent experiments. Student t-test was used. Bars, mean + SE. *$p<0.05$; **$p<0.01$; ****$p<0.0001$, NS, not significant.

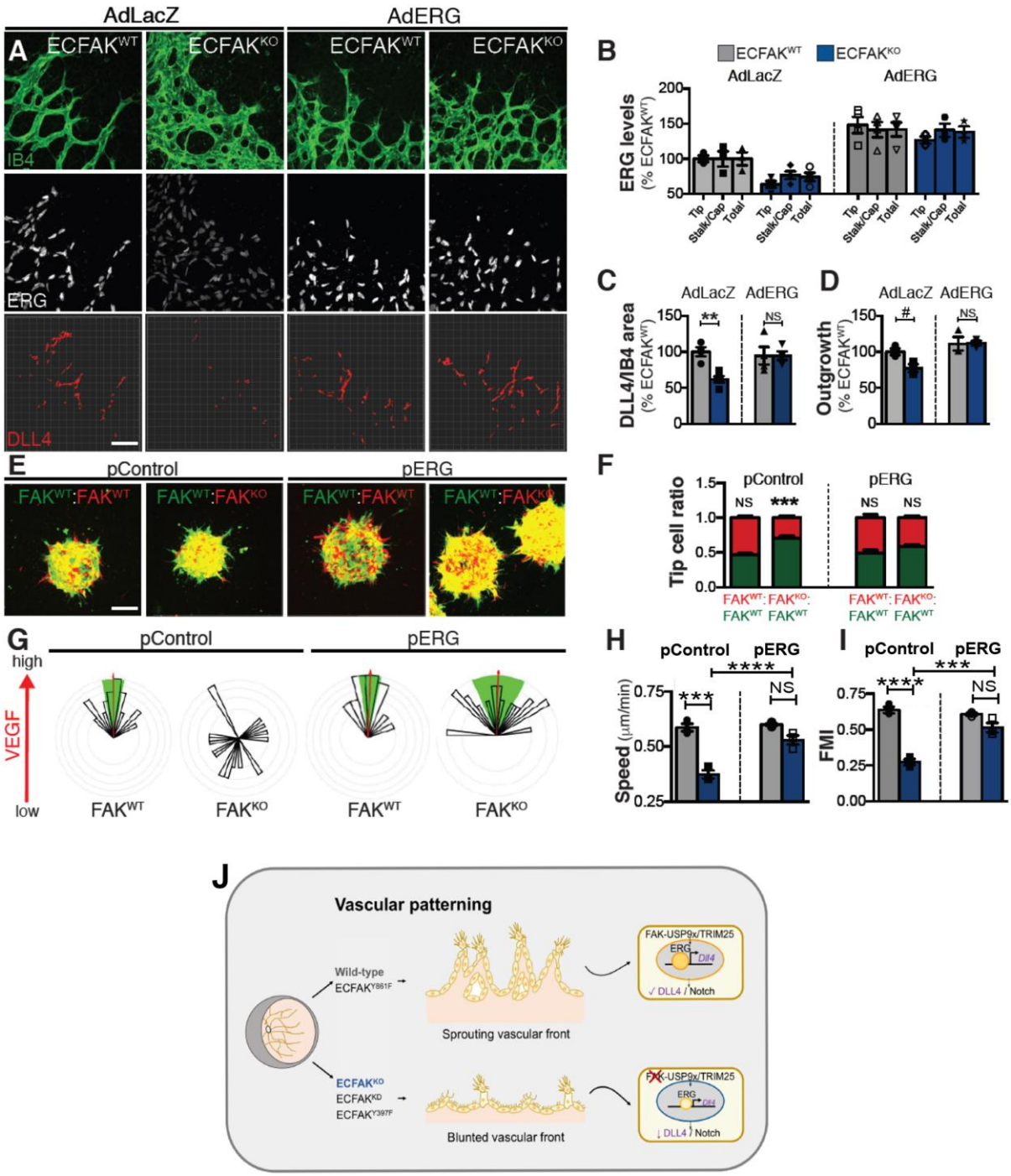

Fig 5. ERG re-expression in ECFAK^{KO} restores DLL4 levels and vascular outgrowth *in vivo* and tip-cell positioning and directed chemotactic migration *in vitro*. (**A**) IB4/ERG/DLL4 triple-stained retinal fronts and quantitation. Scale bars: 50 μm. (**B**) ERG and (**C**) DLL4 in Adeno-LacZ (AdLacZ) or Adeno-ERG (AdERG) P6 ECFAK^{WT} and ECFAK^{KO} pups transduced *in vivo*. (**D**) Vascular outgrowth analysis. *n*: 3 mice per genotype.

Two-Way ANOVA used. (**E**) Representative mages and (**F**) quantitation of sprouting competition assay of FAK^{WT} and FAK^{KO} ECs nucleofected with control (pControl) or ERG (pERG) plasmids *in vitro*. *n*: 10-20 spheroids per condition. Two-Way ANOVA used. Scale bars: 50 μm. (**G**) Dunn chamber chemotaxis, pControl- or pERG-FAK^{WT} and FAK^{KO} ECs. (**H**) Speed and (**I**) FMI analysis. *n*: 3 independent experiments analysing 22-44 cells per condition. Two-Way ANOVA used. **(J)** Schematic shows a model of how ERG regulation by endothelia-cell FAK affects blood vessel development and patterning. Bars, mean + SE. ***p*<0.01; ****p*<0.001; *****p*<0.0001; # 0.0642; NS, not significant.

Table 1. Endogenous mouse FAK knockout/ chicken FAK knockin mutant mice nomenclature.

Mice genotype	Mice nomenclature after Tamoxifen treatment
Pdfgb-iCre^{ERT}-;FAK fl/fl	ECFAK^{WT}
Pdfgb-iCre^{ERT}+;FAK fl/fl	ECFAK^{KO}
Pdfgb-iCre^{ERT}+;FAK fl/fl; R26 FAK$^{WT/WT}$	ECFAK^{KIWT}
Pdfgb-iCre^{ERT}+;FAK fl/fl; R26 FAK$^{KD/KD}$	ECFAK^{KD}
Pdfgb-iCre^{ERT}+;FAK fl/fl; R26 FAK$^{Y397F/Y397F}$	ECFAK^{Y397F}
Pdfgb-iCre^{ERT}+;FAK fl/fl; R26 FAK$^{Y861F/Y861F}$	ECFAK^{Y861F}

Table 2. gRNA targeting sequences

Plasmid name	Target gene	Sequence (5'-3')
CGM35	Usp9x	GTCAGCGATTTTTCCGAGAT
CGM36	Usp9x	TAACAATACTCATCGCCTGG
CGM45	Trim25	ATTGCGGGCATCGGTACGGC
CGM46	Trim25	CGGCGCAGAAGGTCACGAAT

Fig. S1.

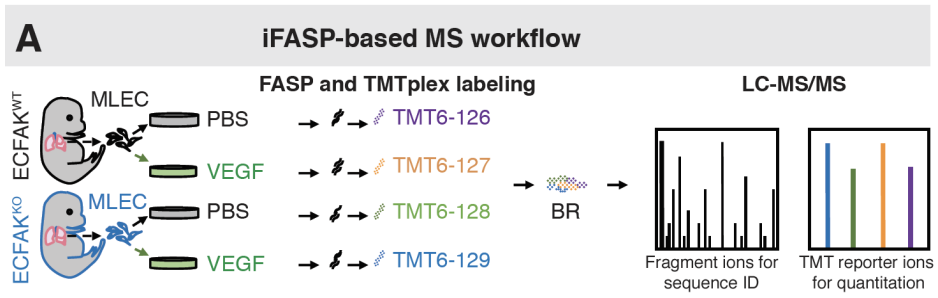

B

	FAK^KO vs FAK^WT	PBS	VEGF
Total	All	174	179
	logFC<0	78	71
	logFC>0	96	108
Phospho	All	87	71
	logFC<0	44	23
	logFC>0	43	48

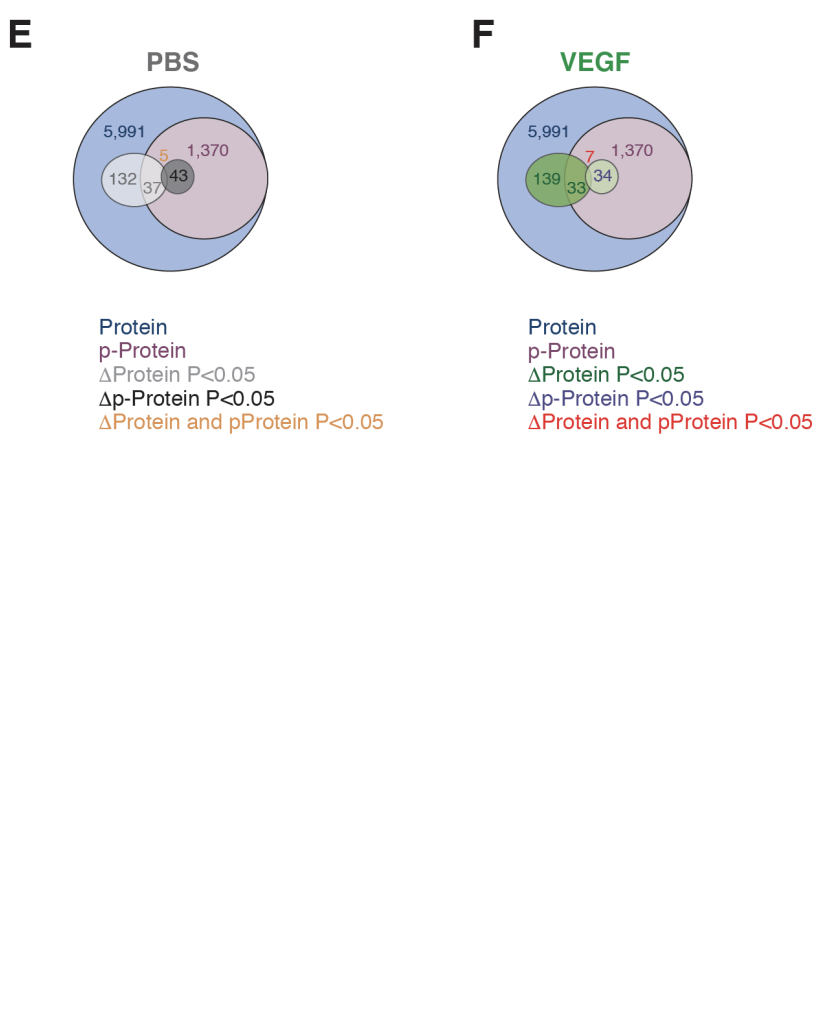

Fig. S1. Phospho-proteomic analysis of primary endothelial cells from ECFAKWT and ECFAKKO neonatal mice. (A) Scheme of workflow of the liquid chromatography-tandem mass spectrometry (LC-MS/MS) proteomic and phospho-proteomic analysis of lung-derived primary endothelial cells isolated ECFAKWT and ECFAKKO mice and stimulated or not with VEGF in vitro. Endothelial cell enriched populations were prepared, from lungs from ECFAKWT and ECFAKKO mice harvested at P10-P14 and expanded by sub-culturing for one passage. Two biological replicates each originated from a pool of three to four lungs of littermate mice of the same genotype. To quantify differential peptide expression levels between wild type (FAKWT) and FAK knock-out (FAKKO) primary endothelial cells PBS control (PBS) and VEGF-stimulated (VEGF), each sample was chemically labelled with isobaric tags for a combined filter-aided sample preparation (FASP) and tandem mass tag (TMT) with multiplexing approach quantification (iFASP) (McDowell et al. 2013). Peptides were then separated, sequenced, and analysed using 2D HPLC tandem high-resolution mass spectrometry (LC-MS/MS) for total phospho-proteome and proteome. **(B)** Table illustrates number of differentially expressed proteins ($p<0.05$, Benjamini-Hochberg test) and number of upregulated ($logFC>0$) or downregulated ($logFC<0$) proteins. **(C)** Proteomic profiling of primary endothelial cells from ECFAKWT and ECFAKKO neonatal mice in PBS and **(D)** VEGF stimulated conditions. Bar charts showing protein category enrichment analysis of differentially regulated proteins in FAKWT and FAKKO endothelial cells in PBS (grey bars) and VEGF (green bars) conditions. Category annotations utilized were from Gene Ontology biological process (GOBP), Gene Ontology cellular component (GOCC), Gene Ontology. molecular function (GOMF), Kyoto Encyclopedia of Genes and Genomes (KEGG) names and Uniprot Keywords databases. Positive enrichment score denotes over-representation, negative enrichment score denotes under-representation. GOBP, GOCC, GOMF, KEGG and Uniprot Keywords terms are displayed, the associated Benjamini-Hochberg corrected p values are provided in deposited datasets. Venn diagrams showing overlap of proteome and phosphor-proteome FAK-dependent datasets in **(E)** PBS and **(F)** VEGF conditions. **(G)** Bar charts showing protein category enrichment analysis of differentially regulated p-proteins in FAKWT and FAKKO endothelial cells in PBS control (grey bars) and VEGF (green bars) conditions. Category annotations utilized were from Gene Ontology biological process (GOBP), Gene Ontology cellular component (GOCC), Gene Ontology molecular function (GOMF), Kyoto Encyclopedia of Genes and Genomes (KEGG) names and Uniprot Keywords databases. Positive enrichment score denotes over-representation, negative enrichment score denotes under-representation. Selected representative Uniprot Keywords terms are displayed, the associated Benjamini-Hochberg corrected p values are provided in deposited datasets.

Fig. S2.

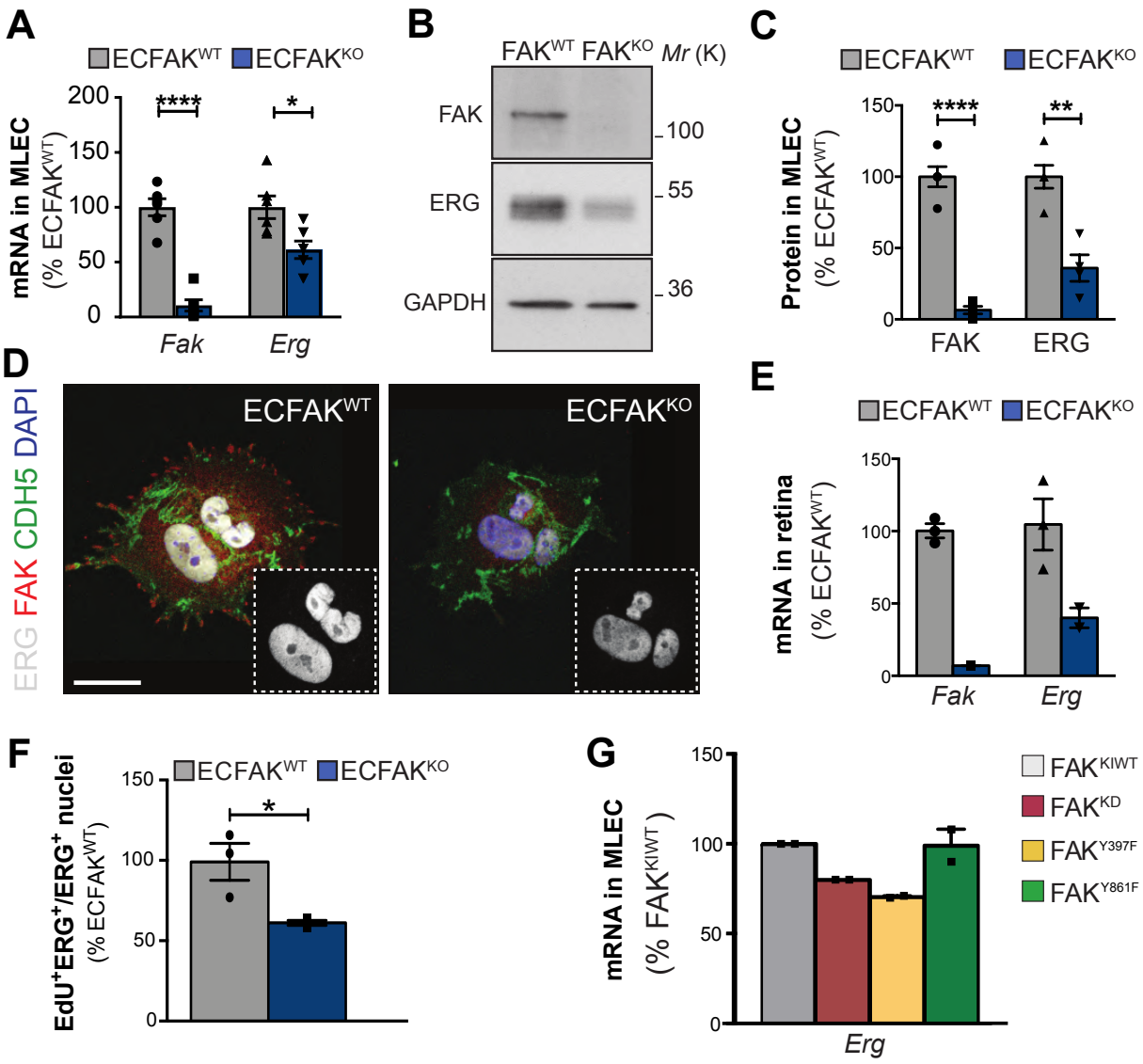

Fig. S2. Endothelial-cell FAK-deficiency, FAK-kinase dead and FAK-Y397F mutations downregulates Erg expression in vivo but FAK-Y861F mutation does not. (A) Transcript levels of Fak and Erg in freshly isolated primary lung ECs from P6 ECFAK^{WT} and ECFAK^{KO}. *n:* 6 independent preparations. Statistical test, Student t-test. **(B)** Western blot analysis and **(C)** densitometry quantitation of freshly isolated primary lung EC lysates show reduction of FAK and ERG expression in P6 ECFAK^{WT} and ECFAK^{KO} samples. GAPDH acts as control. *n:*2 independent EC preparations/genotype; 2-4 pups/genotype/EC preparation. Statistical test, Student t-test. **(D)** Immunofluorescence for ERG, FAK, VE-Cadherin (CDH5) and DAPI in freshly isolated primary lung ECs from ECFAKWT and ECFAKKO pups. Dashed boxes, high magnification showing ERG-stained nuclei. **(E)** qRT-PCR analysis of Fak and Erg transcripts in whole retinal tissue samples from P6 ECFAKWT and ECFAKKO mice. Transcript expressions normalized to CD31/Pecam1, relative to ECFAKWT. *n:*2-3 samples/genotype. **(F)** Retinal endothelial cell proliferation was examined by quantifying the number of double EdU- and ERG-positive cells relative to the total ERG-positive endothelial cell nuclei present in the angiogenic vascular front from ECFAK^{WT} and ECFAK^{KO} retinas. *n:*3. Student t-test used. **(G)** qRT-PCR analysis of primary endothelial cells isolated from P6 ECFAK^{KIWT}, ECFAK^{KD}, ECFAK^{Y397F} and ECFAK^{Y861F} pups. *n:*2 independent endothelial cell preparations for each ECFAKKI genotype. Each endothelial cell preparation consisted of a pool of 2-4 lungs of 4-OHT treated pups of same genotype. Note: endothelial cell lysates for mRNA isolation and western blot analysis, and endothelial cells utilized for immunofluorescence were made without culturing the cells to reflect the *in vivo* mRNA and protein levels as closely as possible. Bars, mean +/- SE. **p<0.01, ***p<0.001, NS: not significant. Scale Bars, 10 μm.

Fig. S3.

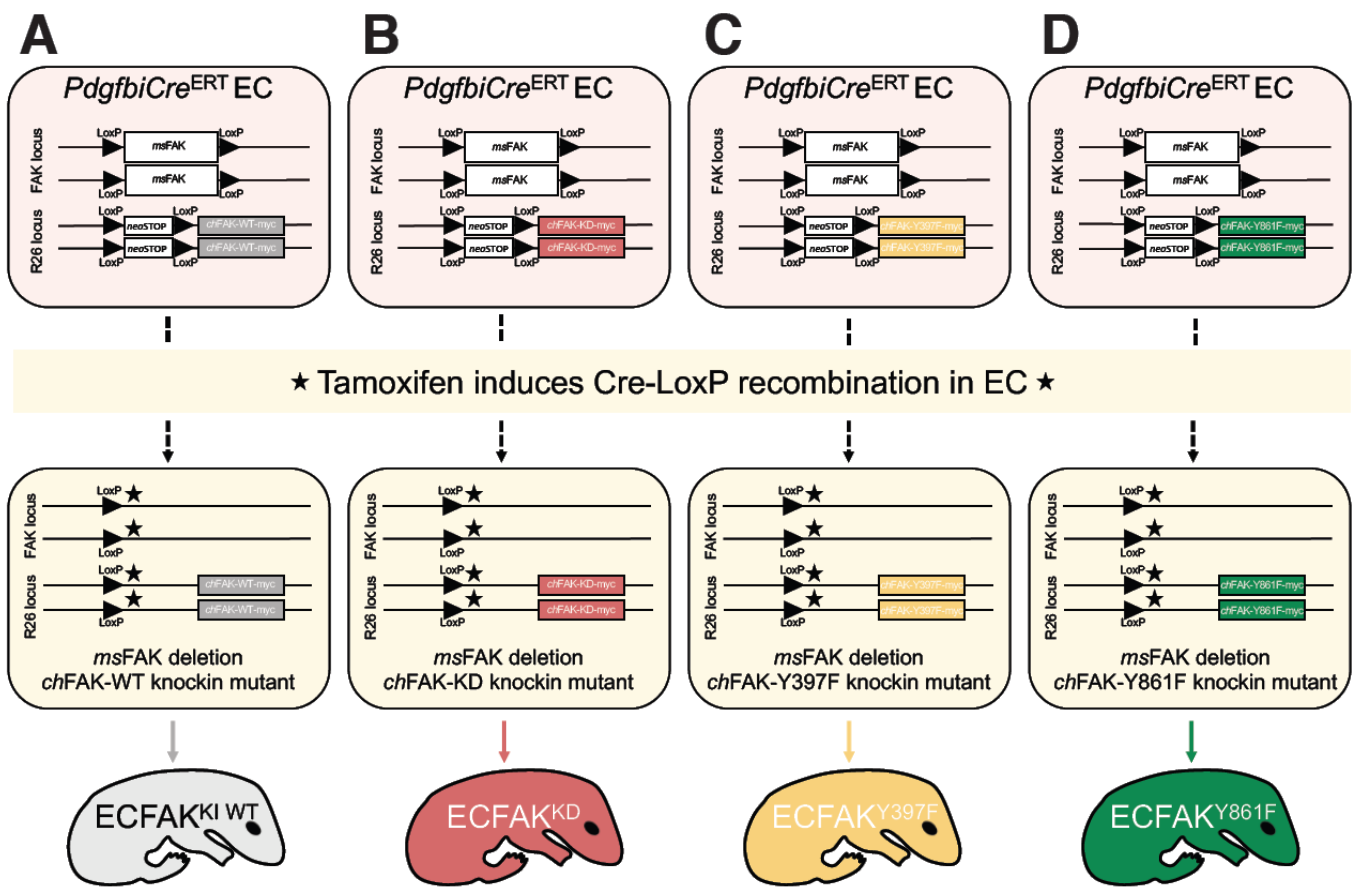
A
B
C
D
PdgfbiCreERT EC
FAK locus
R26 locus
LoxP
msFAK
neoSTOP
chFAK-WT-myc
chFAK-KD-myc
chFAK-Y397F-myc
chFAK-Y861F-myc
★ Tamoxifen induces Cre-LoxP recombination in EC ★
msFAK deletion
chFAK-WT knockin mutant
msFAK deletion
chFAK-KD knockin mutant
msFAK deletion
chFAK-Y397F knockin mutant
msFAK deletion
chFAK-Y861F knockin mutant
ECFAKKI WT
ECFAKKD
ECFAKY397F
ECFAKY861F

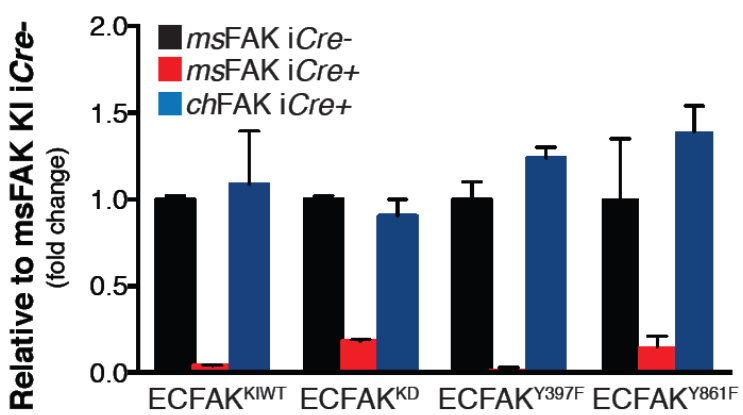
E
Relative to msFAK KI iCre-
(fold change)
msFAK iCre-
msFAK iCre+
chFAK iCre+
2.0
1.5
1.0
0.5
0.0
ECFAKKIWT
ECFAKKD
ECFAKY397F
ECFAKY861F

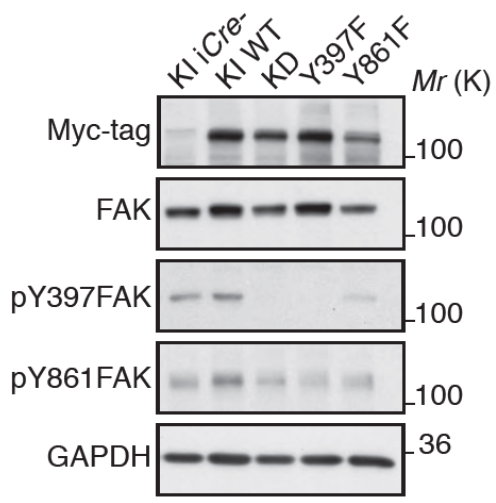
F
KI iCre-
KI WT
KD
Y397F
Y861F
Mr (K)
Myc-tag
FAK
pY397FAK
pY861FAK
GAPDH
100
100
100
100
36

Fig. S3. Validation of FAK knockout/knockin system in vivo and in vitro. PdgfbiCreERT; FAK fl/fl mice (Tavora et al.2010) were intercrossed with mutant chicken FAK knockin mice (Tavora et al. 2014) to generate: PdgfbiCreERT;FAKfl/fl;R26FAKWT/WT; PdgfbiCreERT;FAKfl/fl;R26FAKKD/KD; PdgfbiCreERT;FAKfl/fl;R26FAKY397F/Y397F and PdgfbiCreERT;FAKfl/fl; R26FAKY861F/Y861F genotypes. Endogenous FAK is floxed and knockin chicken-FAK mutants were produced as homozygotes. Administration of tamoxifen induces Pdgfb-driven activation of Cre recombinase leading to simultaneous deletion of the endogenous mouse (ms) FAK gene and the neoSTOP cassette thus allowing the homozygous expression of the myc-tagged mutated chicken (ch) FAK transgene wild-type (KIWT), kinase dead (KD), non-phosphorylatable Y397 (Y387F) or non-phosphorylatable Y861 (Y861F) knockin-chicken-FAK expression specifically in endothelial cells to generate **(A)** ECFAKKIWT, **(B)** ECFAKKD **(C)** ECFAKY397F and **(D)** ECFAKY861F mice, respectively. Tamoxifen induction schedule used in this study is described in Methods. **(E)** For validation of FAK knockout/knockin strategy in vivo: primary endothelial cells were isolated from P6 pups that were treated at P1 and P2 with 4-OHT. Note: endothelial cell lysates for mRNA isolation were made without culturing the cells to reflect the in vivo mRNA levels as closely as possible. Endogenous (mouse) and chicken (knockin) mRNA FAK levels relative to Pecam1 mRNA levels - as an EC purity control - were assessed by qRT-PCR. (n:2-3 independent endothelial cell preparations for each ECFAKKI genotype. Each endothelial cell preparation consisted of a pool of 2-4 lungs of 4-OHT treated pups of same genotype. Bars, mean +/- SE (relative to endogenous msFAK mean expression in ECFAKKI iCre- corresponding control). **(F)** For validation of FAK knockout/knockin strategy in vitro: Western blot analysis of lysates from immortalized lung EC isolated from ECFAKKIWT; ECFAKKD, ECFAKY397F and ECFAKY861F mice. All iCre+ lines express Myc-tag as expected; pY397 is reduced in FAKKD and FAKY397F lysates, but less in FAKY861F lysates; pY861 is reduced in all FAK-mutants. GAPDH acts as loading control.

Fig.S4.

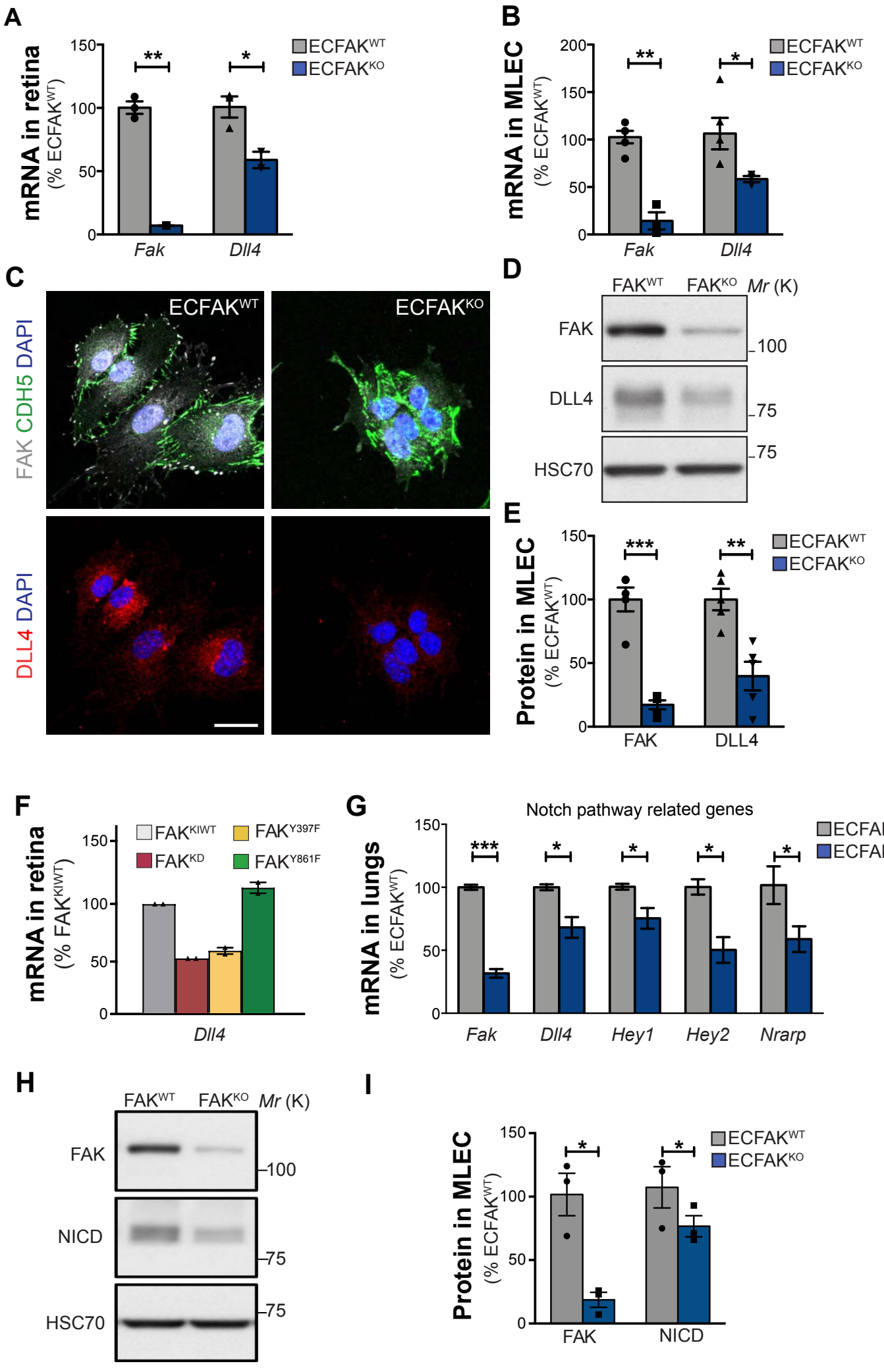

Fig. S4. Endothelial-cell FAK regulates DLL4 and Notch signaling effectors expression *in vivo*. (**A**) mRNA expression of *Fak* and *Dll4* levels from whole retinal tissue from P6 ECFAKWT and ECFAKKO reveals reduced expression of *Fak* and *Dll4* transcripts in ECFAKKO samples. Transcript expression is normalized to *CD31*/*Pecam1*, relative to ECFAKWT. *n:*2-3 samples/genotype; 4-6 retinas/genotype/sample. (**B**) Transcript levels of *Fak* and *Dll4* in freshly isolated primary ECs from ECFAKWT and ECFAKKO pups. *n:*3-5 independent EC preparations/experiment. Student's t-test used. (**C**) Immunofluorescence for DLL4, FAK, VE-Cadherin (CDH5) and DAPI in freshly isolated primary ECs from ECFAKWT and ECFAKKO pups. (**D**) Western blot analysis and (**E**) densitometric quantitation of FAK and DLL4 protein levels from lung derived ECs from ECFAKWT (FAKWT) and ECFAKKO (FAKKO) mice. Student's t-test used. *n:* 5 independent EC preparations/experiment. Student's t-test used. (**F**) qRT-PCR analysis of primary endothelial cells freshly isolated from P6 ECFAKKIWT, ECFAKKD, ECFAKY397F and ECFAKY861F pups. *n:*2 independent endothelial cell preparations for each ECFAKKI genotype. Each endothelial cell preparation consisted of a pool of 2-4 lungs of 4-OHT treated pups of same genotype. (**G**) mRNA expression analysis for Notch signaling effectors *Dll4*, *Hey1*, *Hey2* and *Nrarp* qRT-PCR on whole lung lysates isolated from P5 ECFAKWT and ECFAKKO mice. Deletion of endothelial FAK was induced *in vivo* by administering 4-OHT at P1 and P2. *n:2* ECFAKWT mice and *n:3* ECFAKKO littermate mice, 3 replicates per sample. Note: endothelial cell lysates for mRNA isolation and western blot analysis, and endothelial cells utilized for immunofluorescence were made without culturing the cells to reflect the *in vivo* mRNA and protein levels as closely as possible. **(H)** and **(I)** Western blot analysis of FAK and Notch intracellular domain (NICD) expression protein levels in immortalized lung-derived endothelial cells from ECFAKWT (FAKWT) and ECFAKKO (FAKKO) mice. HSC70 acts as loading control. n:3 independent EC preparations/experiment. Bars, mean +/- SE. * $p<0.05$, **$p<0.01$, ***$p<0.001$, NS: not significant. Scale Bars, 10 μm.

Fig.S5.

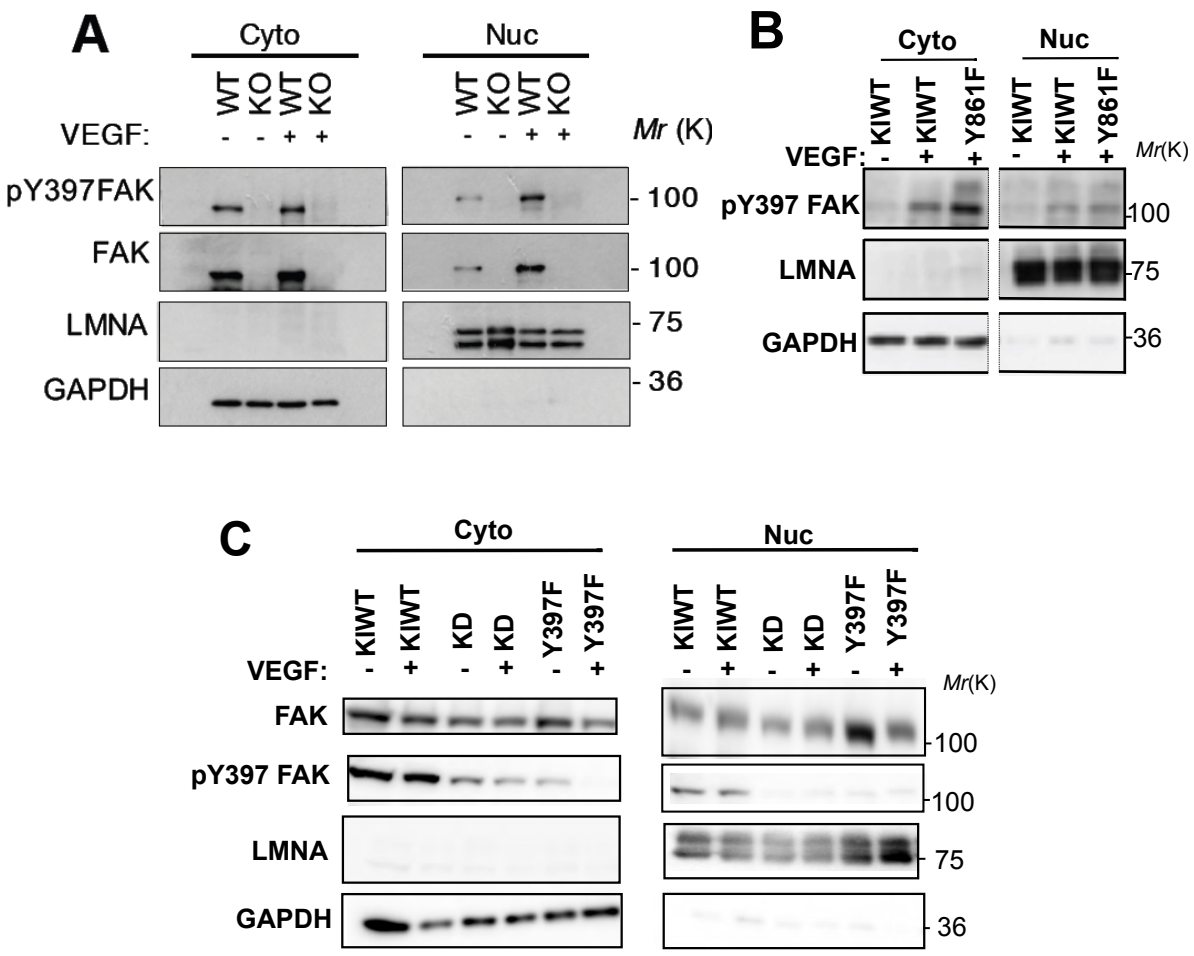

Fig. S5. Full-length wild-type and KD, Y397F and Y861F mutants of endothelial-cell FAK translocate to the nucleus in presence of VEGF. (A) Subcellular fractionation and Western blot analysis of cytoplasmic (Cyt) and nuclear (Nuc) fractions of lung-derived primary endothelial cells isolated from P6 ECFAKWT and ECFAKKO mice and stimulated with VEGF (50 ng/ml) for 30 min in vitro. and **(C)** lung-derived primary endothelial cells isolated from P6 **(B)** ECFAK^{KIWT} and ECFAK^{Y861F} and (C) ECFAK^{KIWT}, ECFAK^{Y397F} and ECFAK^{KD} and mice and stimulated with VEGF (50 ng/ml) for 30 min in vitro. n: 2 independent endothelial cell preparations for each genotype.

Fig.S6.

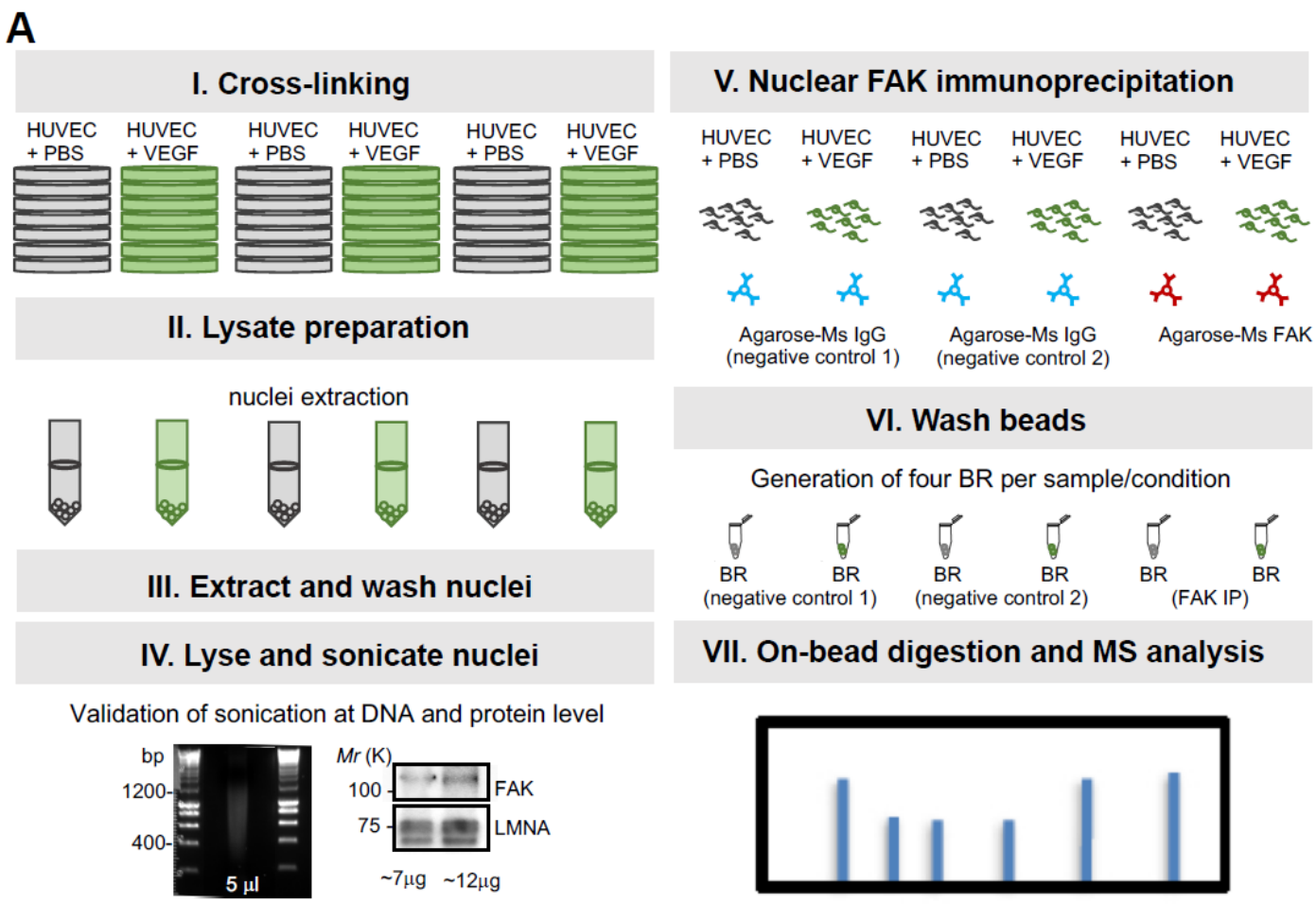

Fig. S6. Nuclear ECFAK interactome in the context of ERG transcription factor. (A) Scheme of the workflow for Rapid Immunoprecipitation Mass spectrometry of Endogenous proteins (RIME) approach used to identify nuclear endothelial-cell FAK interactome. n: 25 biological replicates of protein lysates extracted from Human Umbilical Vein Endothelial Cells (HUVEC) that were stimulated with PBS (vehicle control, n:15) or VEGF (n:10). See Materials and Methods for details.

Fig.S7.

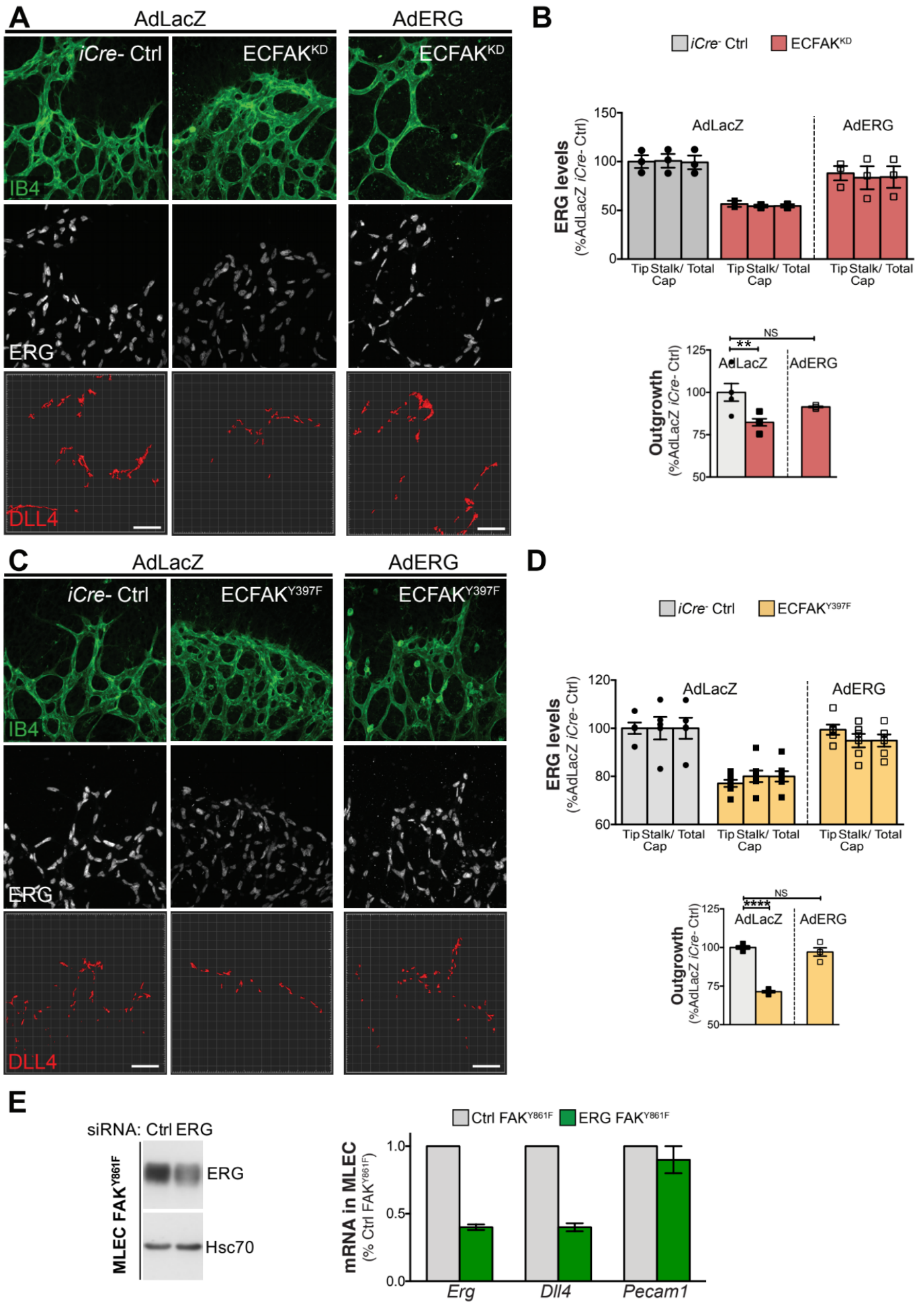

Fig. S7. Expression of ERG in ECFAK^{KD} and ECFAK^{Y397F} mice is sufficient to restore DLL4 expression and vascular outgrowth. (A) Confocal microscopy images of whole mount retinas immunostained for IB4, ERG and DLL4 from P6 Cre-negative controls (iCre- Ctrl) and ECFAKKD pups treated with AdLacZ or AdERG viruses. **(B)** Immunofluorescence quantitation of ERG and DLL4 expression in vivo in P6 iCre- Ctrl and ECFAKKD retinas after pup infection with AdLacZ or AdERG. Quantitation of retinal vascular outgrowth. n:3-4 pups/genotype/Ad-treatment. One-Way ANOVA test used. **(C)** Confocal microscopy images of whole-mount retinas immunostained for IB4, ERG and DLL4 from P6 iCre- Ctrl and ECFAKY397F mice treated with AdLacZ or AdERG virusesent **(D)** Immunofluorescence quantitation of ERG and DLL4 expression in P6 iCre- Ctrl and ECFAKY397F retinas after pup infection with AdLacZ or AdERG. Quantitation of retinal vascular outgrowth. *n*:4-6 pups/genotype/Ad-treatment. One-Way ANOVA test used. **(E)** Western blot analysis shows substantial reduction of ERG protein after ERG-specific siRNA transfection. Bar charts represent transcript analysis of Dll4, ERG and PECAM1 expression levels in FAKY861F ECs. n:2 independent experiments. Bars, mean + SE. **p<0.001; ****p<0.0001 and NS, not significant. Scale bars, 50 μm.

Fig.S8.

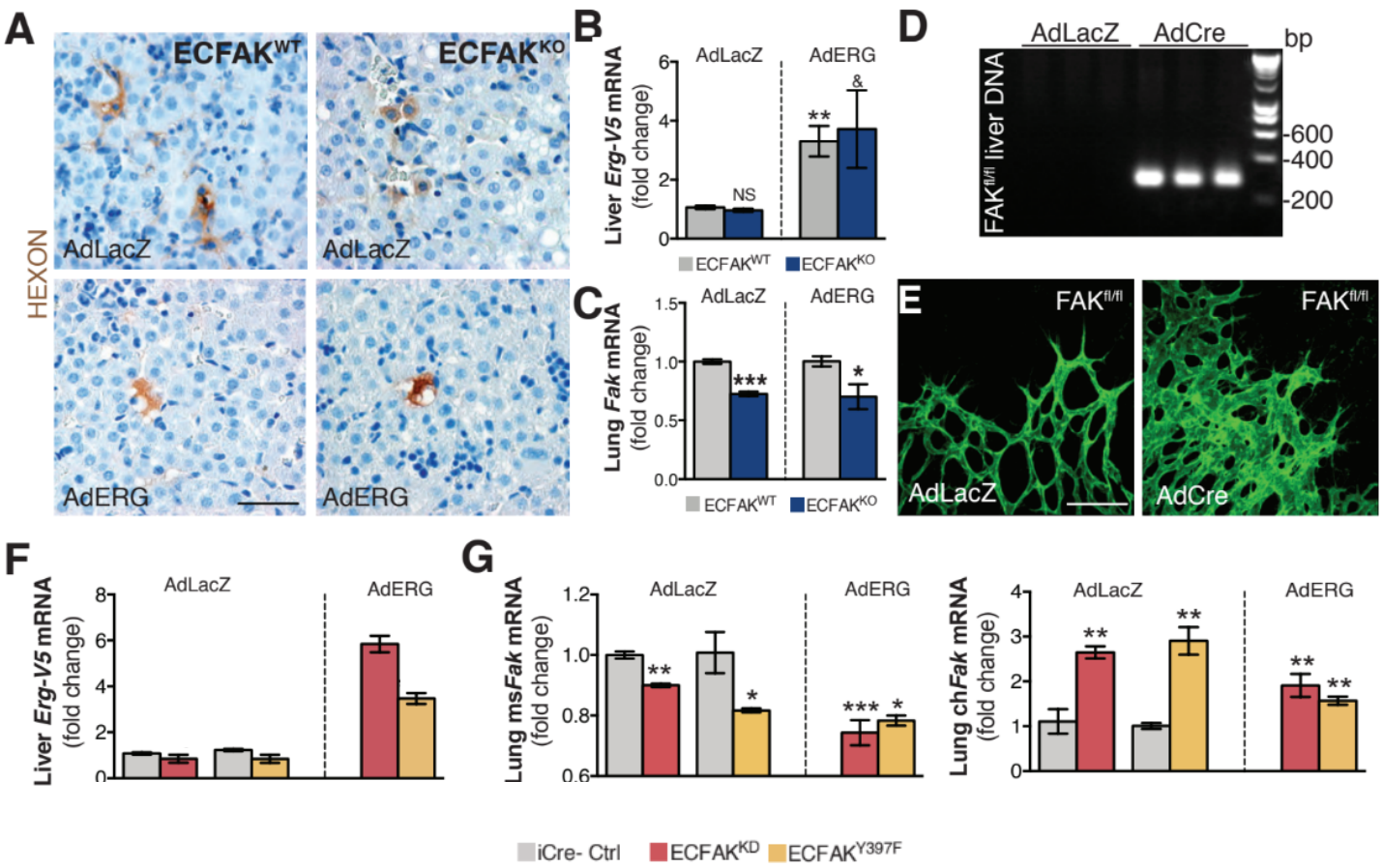

Fig. S8. Validation of the adenoviral-mediated gene expression in vivo strategy and ERG expression after Adeno-ERG transduction in vivo. **(A)** Hexon immunohistochemistry in livers from ECFAK^{KO} Adeno-treated pups. Images show chromogenic DAB immunohistochemistry in livers from ECFAKWT and ECFAK^{KO} pups stained for Hexon (brown), major coat protein in adenoviruses. Scale Bar, 100 Pm. **(B)** Quantitation of qRT-PCR for V5-Erg in livers from AdenoLacZ (AdLacZ) or AdenoERG (AdERG) infected ECFAK^{WT} and ECFAK^{KO} pups at postnatal day (P) that were subsequently administered 4-OHT tamoxifen (at P2 and P3). *n:*5 mice for ECFAK^{WT} and N=5 for ECFAK^{KO} for each Adeno-treated group. **(C)** FAK expression in ECFAK^{KO} treated with AdLacZ or AdERG. *n:*3-4 mice for ECFAK^{WT} and *n:*3 for ECFAK^{KO} for each Adeno-treated group. **(D)** PCR analysis of DNA isolated from P6 livers from AdCre and AdLacZ treated pups. Cre product: 341 bp. **(E)** Confocal microscopy images of IB4 stained retinas from FAK flox/flox AdCre and AdLacZ treated pups at P6. Scale Bar, 50 Pm. **(F)** Qrt PCR for V5-Erg in livers from AdenoLacZ- or AdenoERG-treated at postnatal day (P1) ECFAKKI mice that subsequently were administered 4-OHT tamoxifen at P2 and P3. n:2 mice for ECFAKKI iCre- and *n:*3 for ECFAKKI iCre +. **(G)** mRNA expression analysis for endogenous mouse (knockout) FAK by qRT-PCR in total lung lysates from AdenoLacZ- or AdenoERG-treated as in (F). *n*:3 mice for ECFAKKI iCre- and *n:*3 for ECFAKKI iCre+ for each Adeno-treated group. Bars, mean values +/- SE. One Way ANOVA used. * p<0.05, **p<0.001; ****p<0.0001 and NS, not significant.